Water mass properties and exchange between the Nordic seas and the northern North Atlantic during the period 23–6 ka: Benthic oxygen isotopic evidence

Marius Y. Meland,[1,2] Trond M. Dokken,[1] Eystein Jansen,[1,2] and Kjersti Hevrøy[2,3]

Received 11 January 2007; revised 28 September 2007; accepted 29 October 2007; published 21 February 2008.

[1] Twenty benthic oxygen isotope records from different water depths in the Nordic seas and the North Atlantic are compared. During the Last Glacial Maximum, brine formation on continental shelves produced Brine Shelf Water (BSW), sinking below 1500 m in the Nordic seas. Open-ocean convection in the Nordic seas produced Glacial North Atlantic Intermediate Water (GNAIW). GNAIW overflowed the Greenland-Scotland Ridge and entrained depths above and at least partly below 2000 m in the North Atlantic. During the early deglaciation, BSW-enriched intermediate water masses in the Nordic seas were formed. These overflowed the Greenland-Scotland Ridge and influenced the North Atlantic intermediate and deepwater masses. In the Bølling-Allerød (BA), open-ocean convection increased and produced intermediate water in the Nordic seas, with outflow to the North Atlantic. However, deep water with modern characteristics did not entrain water below 2000 m in the North Atlantic in similar amounts as during the Holocene. A new period of brine formation during the Younger Dryas transported BSW to intermediate water masses in the Norwegian Sea. There was also open-ocean convection and meridional overturning in the Nordic seas, but it was probably reduced compared to the BA. In the early Holocene and mid-Holocene, meridional overturning appears similar to that of today. Potential locations for large-scale formation of BSW might have been broad and shallow (<200 m) areas of the North Sea, northeast of Greenland, and north of east Siberia. These settings should be favorable for BSW formation during cold periods.

Citation: Meland, M. Y., T. M. Dokken, E. Jansen, and K. Hevrøy (2008), Water mass properties and exchange between the Nordic seas and the northern North Atlantic during the period 23–6 ka: Benthic oxygen isotopic evidence, *Paleoceanography*, *23*, PA1210, doi:10.1029/2007PA001416.

1. Introduction

[2] The Nordic seas and the high-latitude North Atlantic are important areas for ocean circulation. Inflow of warm Atlantic surface/subsurface water into the Nordic seas, open-ocean convection in the Nordic seas, and returning overflow across the Greenland-Scotland Ridge, form the northern limb of the Atlantic meridional overturning circulation (AMOC). The strength and signature of the AMOC is indirectly reflected in water mass properties, such as temperatures, salinities and oxygen content, both north and south of the Greenland-Scotland Ridge. Overflow water mass forms the lower part of the North Atlantic Deep Water (NADW) in the North Atlantic. Northwardly advected Atlantic Water brings heat to northern Europe and is, in part, responsible for winter air temperatures of the central and eastern Nordic seas being 10°–20°C higher than the zonal mean [*Drange et al.*, 2005]. The strength of southward bottom water flow across the Greenland-Scotland Ridge may thus indirectly be an important contributor to the climate of the Nordic seas and the surrounding landmasses [*Hansen et al.*, 2004].

[3] In the past, water mass properties and exchange across the Greenland-Scotland Ridge probably changed in a significant way. These changes should be detectable in water mass properties at different depths in the Nordic seas and the North Atlantic. A useful tracer of bottom water mass properties is the $\delta^{18}O_b$ value of benthic foraminifera, as it is controlled by both bottom water temperature and $\delta^{18}O$ of seawater ($\delta^{18}O_w$) [*Shackleton*, 1974].

[4] Previously published benthic oxygen isotope records ($\delta^{18}O_b$) in the Nordic seas oscillate between low and high $\delta^{18}O_b$ values during the last glaciation and deglaciation. During cold stadial events anomalously low benthic oxygen isotope events are observed [*Rasmussen et al.*, 1996; *Vidal et al.*, 1998; *Dokken and Jansen*, 1999]. These events deviate strongly from the global $\delta^{18}O$ ice volume component [*Shackleton*, 1987; *Fairbanks*, 1989; *Liu et al.*, 2004]. Some authors suggest that warming of intermediate and deepwater masses caused these $\delta^{18}O_b$ depletions [*Rasmussen et al.*, 1996; *Bauch et al.*, 2001; *Rasmussen and Thomsen*, 2004]. Others suggest that the $\delta^{18}O_b$ depletions were caused by low-$\delta^{18}O$ meltwater in the surface, which then sank to intermediate and deeper water depths through sea-ice freezing and brine rejection [*Vidal et al.*, 1998; *Dokken and Jansen*, 1999; *Labeyrie et al.*, 2005].

[1]Bjerknes Centre for Climate Research, Bergen, Norway.
[2]Department of Earth Science, University of Bergen, Bergen, Norway.
[3]Now at StatoilHydro Bergen, Bergen, Norway.

Copyright 2008 by the American Geophysical Union.
0883-8305/08/2007PA001416

[5] The aim of this work is to study and update our knowledge about water mass properties through time in the Nordic seas and the northern North Atlantic by use of $\delta^{18}O_b$ records. Knowledge about these water masses is important to constrain past ocean circulation. This circulation had a potential role in explaining rapid climate oscillations during the deglaciation. Some studies are already performed (see Table 1 for references). In our study an important improvement is that we synthesize results from a broader geographical area and depth coverage than previously published. This will improve the robustness of our interpretations compared to previous studies.

2. Methods and Strategy

2.1. Isotope Records and Bathymetric Setting

[6] This paper deals with a reinterpretation of previously published data (16 cores) and interpretation of new data (4 cores). See Table 1 for details. The study compares $\delta^{18}O_b$ records from the North Atlantic and the Nordic seas on 800 to 3700 m depth (Figure 1 and Table 1). Thus a satisfactory geographical and vertical coverage in both ocean basins is obtained. Benthic $\delta^{13}C$ ($\delta^{13}C_b$) and planktonic $\delta^{18}O$ ($\delta^{18}O_p$) records are used to support the interpretation of $\delta^{18}O_b$ signals. The work covers the period from 23 to 6 ka (see section 2.4 for details).

[7] The cores in Figure 1 are, for simplicity and overview, divided into five groups based on depth and location. Group 1 (G1) and group 2 (G2) consist of cores from depths above 2000 m in the eastern and western Nordic seas, respectively. Group 3 (G3) are cores from depths below 2000 m in whole of the Nordic seas. Group 4 (G4) and group 5 (G5) includes cores from depths above and below 2000 m, respectively, in the North Atlantic. The Greenland-Scotland Ridge makes a sill, dividing the G1, G2, and G3 cores in the Nordic seas from the G4 and G5 cores in the North Atlantic.

2.2. Isotope Measurements

[8] The benthic oxygen isotope data presented in this work were measured at *Cibicides wuellerstorfi*, *Cibicides lobatulus*, *Cassidulina teretis*, *Melonis barleeanum* and *Oridorsalis umbonatus*. Planktonic oxygen isotope measurements ($\delta^{18}O_p$) are performed on *Neogloboquadrina pachyderma* sinistral and *Globigerina bulloides* for comparison with $\delta^{18}O_b$ measurements in order to interpret similarities and differences in water masses between surface/subsurface and the bottom water. They are also used for age control (see section 2.4).

[9] The $\delta^{13}C_b$ value of the epibenthic *Cibicides* taxonomic group is regarded as a useful tracer of water mass properties because of its ability to trace $\delta^{13}C$ in bottom water masses [*Duplessy et al.*, 1988; *Mackensen et al.*, 1993; *Curry and Oppo*, 2005]. For the other species used, infaunal microhabitats partly exist, and their carbon isotope compositions are to a varying extent influenced by local pore water composition. Therefore benthic carbon isotopes are not considered for the G1 cores and HM94-34, since the deglacial and glacial intervals are poorly covered by $\delta^{13}C_b$ measurements of the *Cibicides* group.

[10] The isotopic data are reported in ‰ versus PDB. The $\delta^{18}O_b$ values are reported on the corrected *Uvigerina* scale (+0.64‰ for *Cibicides sp.* and *O. umbonatus*, +0.36‰ for *M. barleeanum*, and +0.00‰ for *C. teretis* [*Graham et al.*, 1981; *Duplessy et al.*, 1984; *Jansen et al.*, 1988]).

2.3. Ice Volume Correction

[11] We have chosen to isolate the ice volume component of the oxygen isotopes ($\delta^{18}O_{\text{ice volume}}$), since our purpose is to study a combination of bottom temperature and $\delta^{18}O_w$ reflected in the oxygen isotope signal. The $\delta^{18}O_{\text{ice volume}}$ can be directly tied to change in global sea level associated with large glaciations [*Fairbanks*, 1989]. To calculate $\delta^{18}O_{\text{ice volume}}$, an ice volume component of 1.05‰, suggested by *Duplessy et al.* [2002], is used for the Last Glacial Maximum (LGM). A global LGM sea level 120 m lower than today is suggested [*Fairbanks*, 1989; *Liu et al.*, 2004]. The lowered sea level and ice volume correction is used together with the sea level curve of *Liu et al.* [2004] (Figure 2) to calculate an ice volume component of the oxygen isotope values for different time intervals of the deglaciation. The sea level curve of *Liu et al.* [2004] includes sea level indicators from different locations in the West Pacific region (see the article of *Liu et al.* [2004] for further details). It includes rapid sea level rises which are partly observed in other sea level curves [*Bard et al.*, 1996; *Lambeck and Chappell*, 2001; *Peltier*, 2005; *Peltier and Fairbanks*, 2006]. Thus the choice of sea level curve should be of limited importance. Assuming that 120 m lowered sea level corresponds to 1.05‰ oxygen isotope increase, gives this formula:

$$\delta^{18}O_{\text{ice volume}} = \frac{\text{lowered sea level (m)}}{120 \text{ m}} \times 1.05‰ \quad (1)$$

Then we can use equation (1) to calculate benthic oxygen isotope measurements corrected for ice volume:

$$\delta^{18}O_{b-ivc}(‰ \text{ versus PDB}) = \delta^{18}O_b - \delta^{18}O_{\text{ice volume}} \quad (2)$$

2.4. Chronology and Age Control

[12] The studied time slices are the LGM (23.0–18.6 ka), early deglaciation (ED) (18.6–14.7 ka), Bølling-Allerød (BA) (14.7–13.0 ka), Younger Dryas (YD) (13.0–11.7 ka), the early Holocene (EH) (11.7–8 ka) and the mid-Holocene (MH) (8–6 ka). Except for the transition EH/MH and 6 ka, time boundaries are defined based on abrupt changes and extreme events in the $\delta^{18}O$ record of the North Greenland Ice Core Project (NGRIP) ice core (Figure 3a) and the MD99-2284 core (LGM/ED boundary). The transition EH/MH is defined based on an approximate transition to a Holocene warming well documented from many different archives [*Koç et al.*, 1993; *Nesje and Dahl*, 1993; *Andersen et al.*, 2004].

[13] Age models are constructed based on a combination of four different techniques. First, abrupt sea surface/subsurface warmings and coolings (based on foraminifera and diatom assemblages) are found in different cores (Tables 2a and 2b), and are assumed to occur synchronously with similar events in the NGRIP ice core. We assume that there

Table 1. Core Positions, Water Depths, Modern Bottom Temperatures and Salinities, and Sources of Stable Isotope Records, Radiocarbon Measurements, Ash Layers, Percent Nps Distribution and SST Data[a]

Core	Group	Lon	Lat	Water Depth, m	Modern T_{bottom} JAS, °C	Modern S_{bottom} JAS, °C	Reference Benthic Isotopes[b]	Reference Planktonic Isotopes[b]	Laboratory Source $\delta^{18}O$ and $\delta^{13}C$[c]	Reference AMS ^{14}C[b]	Vedde Ash Identified[b]	Saksunarvatn Ash Identified[b]	SST or Percent Nps Data Produced[b]	Time Interval Studied, ka
HM79-6/4	G1	2.55	63.10	900	−0.6	34.91	1	1	UOB	12	12	12	12	6–16
ENAM93-21	G1	−4.00	62.74	1020	−0.6	34.91	18	18	GIF	17	17	17	17	8–23
MD95-2011	G1	7.64	66.97	1048	−0.7	34.91	19	19	UOB	19	7	NI	19	6–14
MD95-2010	G1	4.56	66.68	1226	−0.7	34.91	5	5	UOB	5	5	NI	1	11–23
MD99-2284	G1	−0.98	62.37	1500	−0.9	34.92	1	1	UOB	1	1	1	1	6–23
PS2644	G2	−21.77	67.87	778	−0.6	34.91	25	25	UOK	25	25	NI	25	10–23
JM96-1228	G2	−26.10	67.03	1079	−0.8	34.92	8	8	UOB	8	8	NI	8	9–23
M23062	G3	0.10	68.43	2244	−0.9	34.92	26	26	UOK	27	NI	NI	NP	6–22
PS1243	G3	−6.55	69.37	2711	−0.9	34.91	2	2	UOK	2	2	NI	2	6–23
HM52-43	G3	0.73	64.26	2781	−1.0	34.91	24	24	UOB	24	24	NI	24	6–22
HM94-34	G3	−2.54	73.77	3004	−1.1	34.91	1	22	UOB	22	22	NI	1	6–23
BOFS17K	G4	−16.50	58.00	1150	5.2	35.07	14	14	GL	13	NI	NI	15	6–23
M23419	G4	−19.74	54.97	1491	3.9	34.96	11	11	UOK	ND	NI	NI	23	8–23
JM96-1225	G4	−29.29	64.91	1683	3.6	34.96	9	9	UOB	9	9	NI	8	11–23
NA87-22	G5	−14.57	55.50	2161	3.5	34.91	27	6	GIF	6, 27	NI	NI	27	6–23
M17051	G5	−31.98	56.17	2300	3.1	34.97	11	11	UOK	11	NI	NI	23	6–23
V23-81	G5	−16.14	54.03	2393	3.1	34.91	10	10	UOB	3, 4	10	NI	20	6–23
M23415	G5	−19.15	53.33	2475	3.1	34.96	11	11	UOK	11	NI	NI	28	6–23
V29-202	G5	−21.00	60.00	2658	3.0	34.96	15	15	WOOD	16	NI	NI	16	6–23
M17045	G5	−16.65	52.43	3663	2.9	34.96	11	11	UOK	11	NI	NI	23	6–23

[a]SST data refer to foraminifera and diatoms. See section 2.1 for information about the group affiliations. The modern temperature and salinity data are from *Levitus and Boyer* [1994]. Abbreviations are Lon, longitude; Lat, latitude; JAS, July August–September; Nps, *N. pachyderma* (s); AMS, accelerator mass spectrometry; ND, not dated; NI, not identified; and NP, not produced or not used in this work.

[b]Reference sources are 1, this work; 2, *Bauch et al.* [2001]; 3, *Bond et al.* [1993]; 4, *Broecker et al.* [1988]; 5, *Dokken and Jansen* [1999]; 6, *Duplessy et al.* [1992]; 7, *Grönvold et al.* [1995]; 8, *Hagen* [1999]; 9, *Hagen and Hald* [2002]; 10, *Jansen and Veum* [1990]; 11, *Jung* [1996]; 12, *Karpuz and Jansen* [1992]; 13, *Manighetti et al.* [1995]; 14, *Maslin* [1992]; 15, *Maslin et al.* [1995]; 16, *Oppo and Lehman* [1995]; 17, *Rasmussen et al.* [1996]; 18, *Rasmussen et al.* [1998]; 19, *Risebrobakken et al.* [2003]; 20, *Ruddiman and McIntyre* [1981]; 21, *Sarnthein et al.* [1994]; 22, *Sarnthein et al.* [1995]; 23, *Schulz* [1995]; 24, *Veum et al.* [1992]; 25, *Voelker* [1999]; 26, *Vogelsang* [1990]; 27, *Waelbroeck et al.* [2001]; and 28, *Weinelt et al.* [2003].

[c]Laboratory abbrevitions are GL, Godwin Laboratory, Cambridge; GIF, Laboratoire mixte CNRS-CEA, Gif sur Yvette; UOB, University of Bergen; UOK, University of Kiel; and WOOD, Woods Hole Oceanographic Institution.

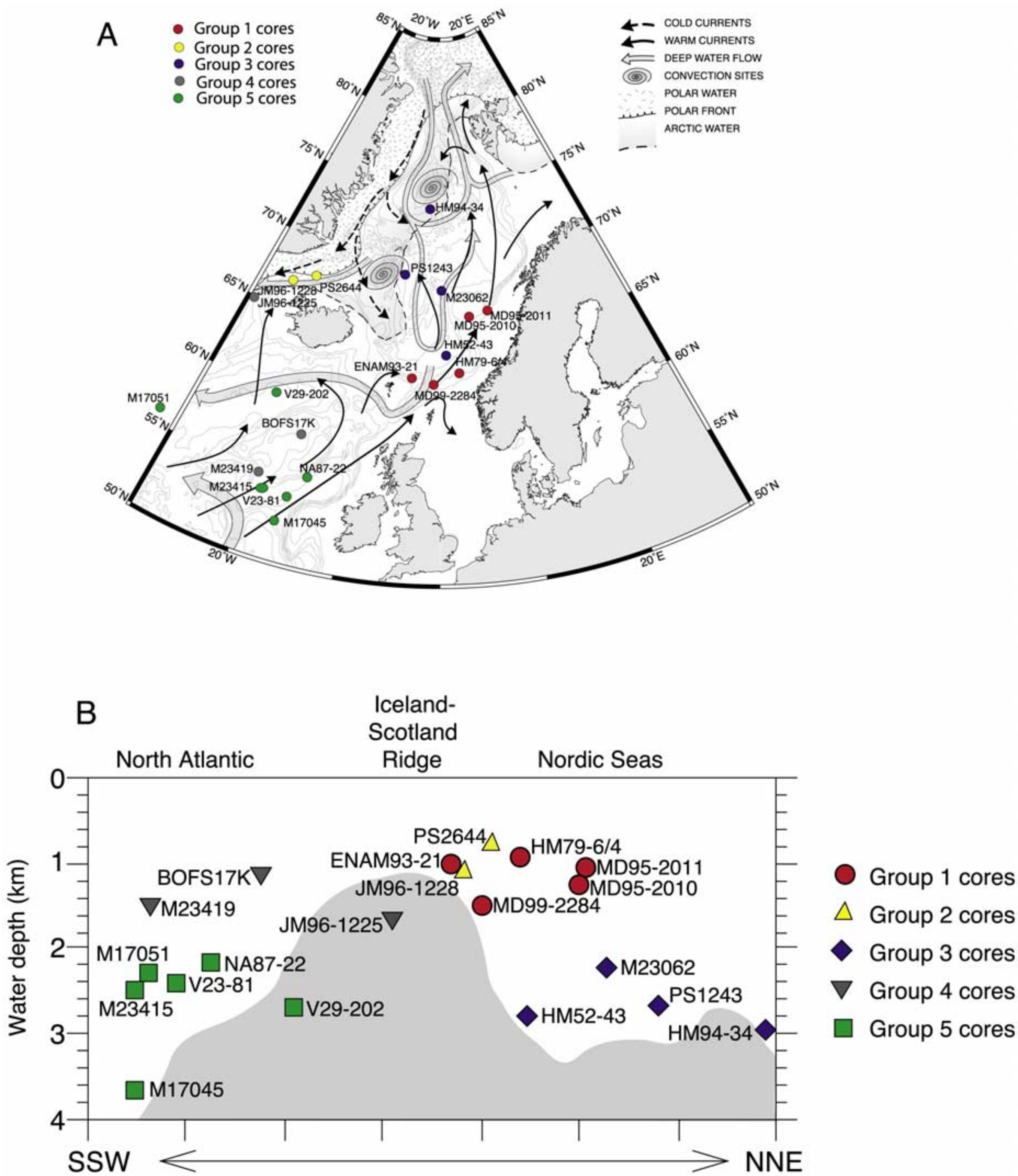

Figure 1. (a) Map of the Nordic seas and the northern North Atlantic with ocean currents, fronts, and bathymetry. The studied cores are shown as circles. The different colors denote the group affiliations (G1–G5, see text for detailed information). (b) Core locations projected horizontally on a vertical ocean transect. The different symbols denote the different group affiliations. The Greenland-Scotland Ridge divides the ocean basins into the North Atlantic in the south and the Nordic seas in the north. The bathymetric features are (highly schematic) shown in grey.

is a tight coupling between atmospheric Greenland temperatures and North Atlantic SST (sea surface temperature), as demonstrated in previous studies [*Atkinson et al.*, 1987; *Duplessy et al.*, 1992; *Björck et al.*, 1996] (Figure 3). Second, ash layers are found to represent confident age markers. As long as there is no age conflict with sea surface/subsurface warmings and coolings, we assume that these layers consist of the Younger Dryas Vedde Ash [*Mangerud*

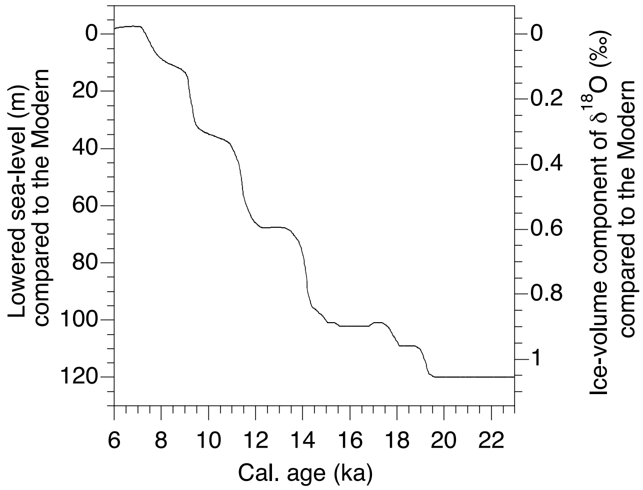

Figure 2. Stepwise postglacial sea level rise [after *Liu et al.*, 2004]. The left *y* axis denotes the lowered sea level compared to the Modern. The right *y* axis denotes the inferred global ice volume component of $\delta^{18}O$ compared to the Modern, calculated from equation (1) in text. The sea level curve does not go beyond 22 ka. For the period 23–22 ka an LGM ice volume component of 1.05‰ is assumed [*Duplessy et al.*, 2002].

et al., 1984] and the early Holocene Saksunarvatn Ash [*Mangerud et al.*, 1986]. Third, planktonic oxygen isotope events in the sediment core MD99-2284 are used to define the end of the LGM and peak melting events during the ED (Tables 2a and 2b). These events are partly found in the other cores, and are assumed to occur synchronously with the events in MD99-2284. See Tables 2a and 2b for details. Last, calibrated ages are calculated in the Calib 5.0 software [*Stuiver and Reimer*, 1993] from previously published accelerator mass spectrometry (AMS) ^{14}C ages.

[14] Calibrated ages based on AMS ^{14}C ages are calculated using a reservoir age of 400 years in Calib 5.0. No other reservoir correction has been used, but there may have been extended reservoir ages for different time slices, mainly the YD and the ED [*Hagen*, 1999; *Waelbroeck et al.*, 2001; *Bondevik et al.*, 2006]. In our study these extended reservoir ages are not used, since different studies about reservoir ages are not consistent for various regions. Instead we have constrained chronologies by use of sea surface/subsurface temperature and meltwater signals during the deglaciation combined with computed calibrated ages, based on AMS ^{14}C, as far as possible. Where age models deviate from calibrated AMS ^{14}C ages, factors like differing reservoir age and/or contamination of younger/older material may influence. Our study will not discuss these deviations in detail.

[15] During the last deglaciation errors in the age model may lead to significant errors in $\delta^{18}O_{b\text{-}ivc}$. We assume that the $\delta^{18}O_{ice\ volume}$ component and our age models are regarded as reasonable. Errors in the $\delta^{18}O_{b\text{-}ivc}$ curves are largest during events with abrupt sea level increases (Figure 2). There may also be arguments that the end of the LGM should be at ~19.5 ka (just before a rapid sea level increase in Figure 2). However, different AMS ^{14}C datings support an end of the LGM closer to 18–19 ka for the North Atlantic. Thus we have chosen to put the end of the LGM at 18.6 ka for this purpose, which marks the last heavy $\delta^{18}O_p$ value before a significant lowering, observed in the MD99-2284 core. This is partly in agreement with the EPILOG group, who defined the LGM to end at ~19 ka [*Mix et al.*, 2001].

[16] The age models used in the present study are displayed in Figure 4. In this work, cores containing at least a few AMS ^{14}C ages, the Vedde and Saksunarvatn ash layers, and resolution higher than 500 years were given priority. However, a few other cores were also included (Table 1) to obtain sufficient geographical and depth coverage.

2.5. Presentation of Isotope Data and Their Behavior in Different Water Masses

[17] The benthic oxygen isotope records are shown in Figure 5. The $\delta^{13}C_b$ and $\delta^{18}O_p$ records are used to support interpretation of the $\delta^{18}O_{b\text{-}ivc}$ records. For better comparison between the different $\delta^{18}O_{b\text{-}ivc}$ and $\delta^{13}C_b$ records, these records are grouped and shown in Figure 6. Different water masses are typically interpreted to be combinations of different $\delta^{13}C_b$ and $\delta^{18}O_{b\text{-}ivc}$ values (Figure 7) [*Kroopnick*, 1980; *Oppo and Lehman*, 1993; *Dokken and Jansen*, 1999]. Thus $\delta^{13}C_b$ brings important complementary information for interpretation of $\delta^{18}O_{b\text{-}ivc}$ values. However, interpretation of water masses based on this criterion is not straightforward, and should be read with caution.

[18] The $\delta^{18}O_{b\text{-}ivc}$ values for each time slice are also averaged and shown on vertical cross sections in Figures 8a–8g. The transition between the different time slices is also shown (Figures 8h–8l). This is done to indicate how water mass properties changed in a vertical view.

3. Water Mass Properties and Exchanges: Results and Paleoceanographic Interpretations

3.1. Low $\delta^{18}O_{b\text{-}ivc}$ Events: Brine Enrichments or Deep/Intermediate Warmings?

[19] Low $\delta^{18}O_{b\text{-}ivc}$ events in the Nordic seas, especially seen during cold periods, we suggest were caused by enrichment of water with low ^{18}O content, because of sinking of brine-enriched meltwater low in $\delta^{18}O_{water}$. This is in agreement with *Dokken and Jansen* [1999], *Vidal et al.* [1998] and *Risebrobakken et al.* [2003]. An alternative could be bottom water warming of about 6°–8°C, in agreement with *Rasmussen et al.* [1996] and *Rasmussen and Thomsen* [2004]. We find the last suggestion not reliable, since inflowing intermediate water would need to attain the density of water masses below 1 km depth (previously formed by convection). Also, even though several model studies document that deep water can be warmed by several degrees [*Weaver et al.*, 1993; *Winton*, 1997; *Paul and Schulz*, 2002], these experiments do not take care of that warm inflowing water has to pass a shallow ridge and fill large parts of the Nordic seas. In addition, low benthic Mg/Ca ratios from core MD95-2010 contradict high temperatures in intermediate water (T. Dokken and X. Clark, unpublished data, 2007).

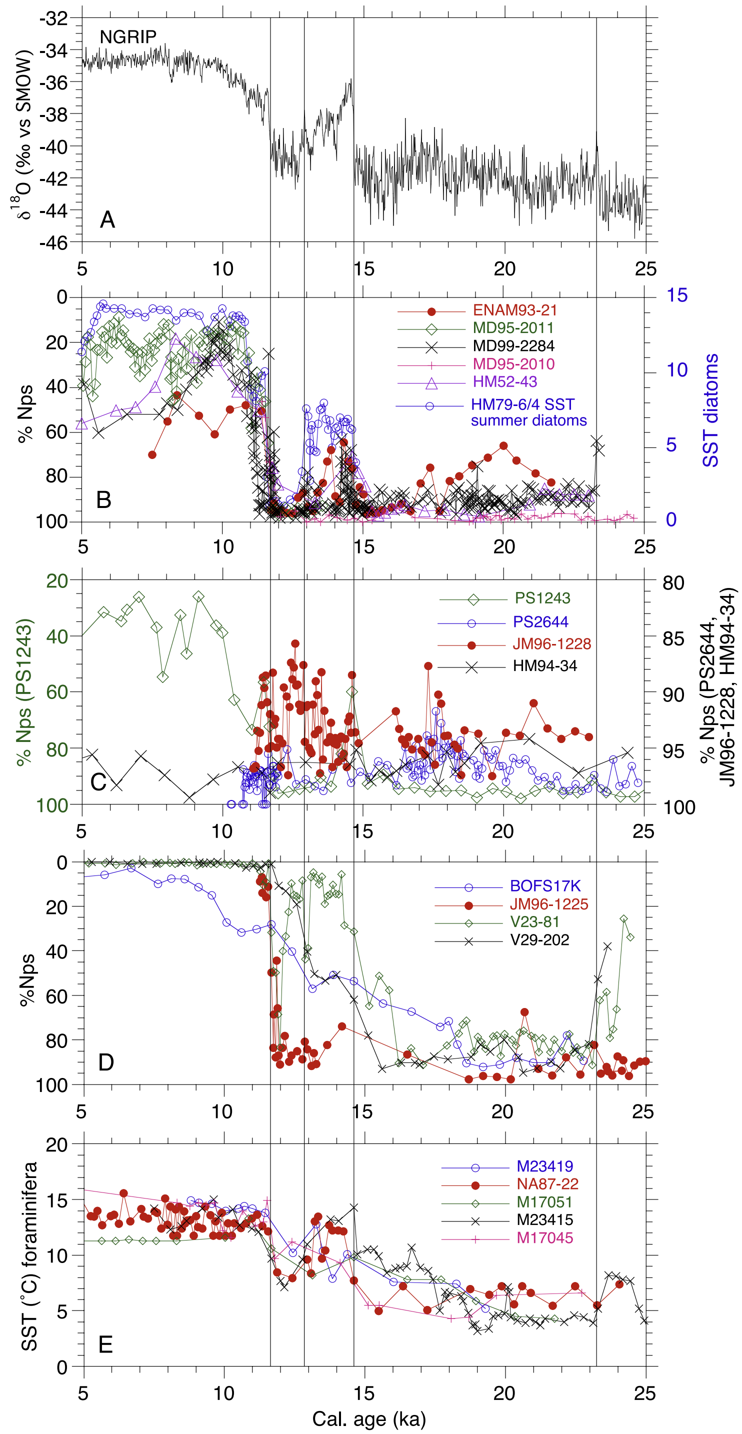

Figure 3. Correlation of different SST (sea surface temperature) records from sediment cores in this study to the North Greenland Ice Core Project (NGRIP) ice δ^{18}O (a proxy for air temperature) [*Rasmussen et al.*, 2006]. Planktonic δ^{18}O records are also used for correlation, primarily for the end of the LGM and meltwater peaks during the ED but are not shown here because of lack of space (see Tables 2a and 2b and the planktonic δ^{18}O records plotted against calendar age in Figure 5 for details). (a) NGRIP ice core [*Rasmussen et al.*, 2006]. The vertical lines refer to stratigraphic markers in the NGRIP and corresponding markers in the percent *N. pachyderma* (s) and SST records Figures 3b–3e. Only a selection of the markers in the NGRIP ice core was found in the SST records (see Tables 2a and 2b for details). SST records and percent *N. pachyderma* (s) distribution records (see Table 1 for references) of (b) the eastern Nordic seas, (c) the western and central Nordic seas, and (d and e) the North Atlantic cores.

Table 2a. Ash Layers and Events From the NGRIP Ice Core (Figure 3a)[a]

Time Marker	Cal Age, ka	Group 1 HM79-6/4	ENAM93-21	MD95-2011	MD95-2010	MD99-2284	Group 2 PS2644	JM96-1228	Group 3 M23062	PS1243	HM52-43	HM94-34	Group 4 BOFS17K	M23419	JM96-1225	Group 5 NA87-22	M17051	V23-81	M23415	V29-202	M17045
1	8.22			F																	
2	10.28	S	S			S															
3	11.67	D	F	F	F	F		F		F	F		F	F	F	F	F	F	F	F	F
4	11.98	V	V	V	V	V	V	V		V	V	V			V			V			
5	12.95	D				F		F					F	F		F			F		
6	14.61	D	F			F		F		F	F		F	F	F	F		F	F	F	F
7	16.50				O		O	O	O		O	O			O		O				
8	18.60		O		O		O	O			O	O	O		O	O	O		O		
9	23.29					F					F							F	F	F	

[a]These events are used for correlation with the sediment cores (Figures 3b–3e). The letters are abbreviations describing the proxies used in the sediment cores for correlation with North Greenland Ice Core Project (NGRIP). Abbreviations are S, Saksunarvatn Ash; V, Vedde Ash; F, foraminiferal SST or percent *N. pachyderma* (s) distribution; D, diatom SST; and O, planktonic oxygen isotopes. Cal stands for calendar.

[20] Thus we suggest that low $\delta^{18}O_{b\text{-ivc}}$ events in the Nordic seas were due to brine enrichment, while low $\delta^{18}O_{b\text{-ivc}}$ events in the North Atlantic may, at least partly, document deepwater warming. This will be discussed more detailed in the following sections 3.2–3.6. Potential areas for intensive brine formation may have been deglaciated broad shallow areas (<200 m water depth) in the North Sea, outside northeastern Greenland and north of the Siberia (Figure 9).

3.2. Last Glacial Maximum (22.8–18.7 ka)

[21] In the eastern Nordic seas high $\delta^{18}O_{b\text{-ivc}}$ values (3.9–4.5‰) are observed at depths above 2000 m (Figures 6 and 8b). The values were approximately similar as today, and suggest modern-like conditions in intermediate water.

[22] In the deeper Nordic seas (>2000 m) the $\delta^{18}O_{b\text{-ivc}}$ values were 0.5–1.5‰ lower than today (Figures 6 and 8b). This difference suggests larger amounts of brine-rich and $\delta^{18}O$-depleted deep water below 2000 m.

[23] At intermediate depths in the western Nordic seas, $\delta^{18}O_{b\text{-ivc}}$ values show a fluctuating pattern, with extremely low values in core JM96-1228 (Figure 6, G2). *Hagen* [1999] explains them with foraminifera reworked from the Greenland continental shelf. However, nearby cores PS2644 and JM96-1225 also show fluctuations, but to a lesser degree. In addition, low $\delta^{18}O_{b\text{-ivc}}$ values in cores JM96-1228, PS2644 and JM96-1225 correspond to lowered $\delta^{13}C_b$ values in these cores, respectively (Figure 6). Therefore we suggest that low $\delta^{18}O_{b\text{-ivc}}$ values were caused by periods with brine injected into intermediate water masses in the western Nordic seas. Since the $\delta^{18}O_{b\text{-ivc}}$ and $\delta^{13}C_b$ fluctuations are higher in the northernmost JM core than the southernmost, we suggest periodically high Brine Shelf Water (BSW) formation in the western Nordic seas, with southward outflow through the Denmark Strait. Potential sites for intermediate water was outside the northeastern Greenland, but possibly also around relatively shallow areas surrounding Iceland (Figure 9).

[24] Brine-enriched bottom water formed from sea ice freezing along glacial continental margins should be mostly depleted in $\delta^{13}C$, because of influence from $\delta^{13}C$-depleted glacial meltwater. Thus we should expect lower $\delta^{13}C_b$ values than shown in the deep Nordic seas (Figure 6, G3). One explanation might be that this deep water contained signatures of ^{13}C-enriched Glacial North Atlantic Intermediate Water (GNAIW), layered above. Thus high $\delta^{13}C_b$ values in the deeper Nordic seas can be reconciled by open-ocean convection in the central Nordic seas causing GNAIW to overlie brine-enriched deep water. Alternatively, glacial meltwater giving this brine signal may of some reason (e.g., ^{13}C-enriched glacial debris) explain the high $\delta^{13}C_b$ values in the deep water. We think a combination of the two hypotheses above is the most probable, since we should expect higher $\delta^{18}O_{b\text{-ivc}}$ values below 2000 m depth if GNAIW was the only contributor to the high $\delta^{13}C$ of this water.

[25] South of the Greenland-Scotland Ridge the $\delta^{18}O_{b\text{-ivc}}$ values were on average 0.4–0.7‰ higher than in the Holocene (Figures 6 and 8b, G4 and G5). This increase corresponds to a temperature decrease of 1.5°–3°C com-

Table 2b. Description of the Stratigraphic Events From Table 2a

Cal Age, ka	Description, With Reference to the NGRIP Ice Core	Characteristics in the Core Data[a]
8.22	cold peak ("8.2 event") Holocene	low SST/high percent Nps/high $\delta^{18}O_{planktonic}$
10.28	Saksunarvatn ash layer	Saksunarvatn ash layer
11.67	abrupt warming: start of the Holocene	abrupt SST increase/percent Nps decrease
11.98	Vedde ash layer	Vedde ash layer
12.95	abrupt cooling: start of the Younger Dryas	abrupt SST decrease/percent Nps increase
14.61	abrupt warming: start of the Bølling-Allerød	high SST, low percent Nps and/or high $\delta^{18}O_{planktonic}$
16.50[b]	peak meltwater event in MD99-2284	low $\delta^{18}O_{planktonic}$ values/meltwater signal
18.60[b]	end of the Last Glacial Maximum observed in MD99-2284	high $\delta^{18}O_{planktonic}$ values before a significant $\delta^{18}O_{planktonic}$ decrease
23.29	abrupt cooling: start of the LGM	abrupt SST decrease/percent Nps increase

[a]Nps is *N. pachyderma* (s).
[b]These ages are correlated to the MD99-2284 sediment core and not the NGRIP ice core.

pared with today [*Shackleton*, 1974]. The $\delta^{13}C_b$ values were highest in the G4 cores (Figure 6), suggesting a strong influence by GNAIW. Below 2000 m in the North Atlantic, a combination of high $\delta^{18}O_{b\text{-}ivc}$ and low $\delta^{13}C_b$ values (Figure 6, G5) could suggest an influence of Southern Ocean Water (SOW), in agreement with *Boyle and Keigwin* [1987], *Oppo and Lehman* [1993] and *Curry and Oppo* [2005]. Further, *Ninnemann and Charles* [2002] showed that LGM $\delta^{13}C_b$ values in the Southern Ocean were 1–1.5‰ lower than during the Holocene at depths below 2000 m. Glacial $\delta^{13}C_b$ values below 2000 m in the North Atlantic were only 0–0.7‰ lower than the Holocene values (Figure 6, G5). On the basis of simple linear mixing relation, we should expect lower $\delta^{13}C$ of water masses below 2000 m in the North Atlantic if SOW entrained these depths. Thus we do not find any clear evidence about large amounts of SOW at depths of 2000–3000 m in the North Atlantic Ocean. We suggest that GNAIW formed in the Nordic seas, and was able to cross the Greenland-Scotland Ridge, entraining the North Atlantic also below 2000 m. This is partly in agreement with $^{231}Pa/^{230}Th$ ratios from the deeper North Atlantic [*Yu et al.*, 1996; *Gherardi et al.*, 2005], which give no clear indication of a shallower SOW during the LGM.

[26] The transition between high- and low-$\delta^{13}C$ water was mainly placed at ~2000 m, but could in periods fluctuate deeper, possibly to about ~2200 m. This is supported by the periodically high $\delta^{13}C_b$ values in core NA87-22 at 2161 m for the LGM (Figure 6, G5).

3.3. Early Deglaciation (18.7–14.7 ka)

[27] Marked depletions of $\delta^{18}O_{b\text{-}ivc}$ at intermediate depths in the southeastern Nordic seas stands out in the records (Figures 6, 8c, and 8h, G1). A depletion centered at ~16.0 ka is most marked, and is delayed by ~500 years compared with planktonic low-isotope peaks (Figure 5, G1). It is in approximate synchrony with a massive iceberg release from Laurentide, deposited in the North Atlantic as Heinrich layer 1 [*Heinrich*, 1988; *Bond et al.*, 1993]. The $\delta^{18}O_p$ depletions at ~16.5 ka are most marked in the G1 cores (Figure 5), indicating that glacial melting was most intensive at the European continental margin. The ice sheets there melted considerably at this time [*Svendsen et al.*, 1996; *Nygård et al.*, 2004; *Knutz et al.*, 2007]. Thus cold surface water freshened, potentially making conditions favorable for large-scale sea ice and BSW formation. We suggest that this water mass were sinking to intermediate depths, giving $\delta^{18}O_{b\text{-}ivc}$ depletions (Figures 6, 8c, and 8h, G1), in agreement with *Vidal et al.* [1998] and *Dokken and Jansen* [1999].

[28] During ~19–17 ka $\delta^{18}O_{b\text{-}ivc}$ and $\delta^{13}C_b$ depletions are also significant in some cores below 2000 m in the Nordic seas and at intermediate depths in the Nordic seas, but of lower amplitudes (Figure 6, G1, G2, and G3). We suggest that intensive BSW formation during still cold conditions were initiated at 19–18 ka outside northeastern Greenland. Intermediate and deep waters in the western and central Nordic seas, respectively, got the largest influence of brine-enriched water during the start of the ED. During later parts of the deglaciation (~17–15 ka) glaciers in Fennoscandia, North Sea and British Isles melted [*Nygård et al.*, 2004; *Knutz et al.*, 2007], and released broad shallow shelf areas in the North Sea, mostly less than 100 m deep during the ED [*Peltier*, 1994]. Until more investigations are performed, it seems like that the North Sea is a potential candidate in explaining large parts of the $\delta^{18}O_{b\text{-}ivc}$ depletions in the G1 cores.

[29] In the intermediate North Atlantic (G4 cores) a peak depletion is observed around ~18 ka (Figure 6, G4). Decreased $\delta^{18}O_{b\text{-}ivc}$ and $\delta^{13}C_b$ values in BOFS17K do not point to brine-enriched intermediate water from the north, since the values are lower than in the G1 cores for ~18 ka. Instead, glacial melting from the British Isles [*Knutz et al.*, 2007] and potential BSW formation at the shallow shelves outside Ireland may allow brine-enriched water to sink to intermediate depths in the North Atlantic.

[30] Later during the deglaciation (~15–17 ka) low $\delta^{18}O_{b\text{-}ivc}$ and $\delta^{13}C_b$ values are observed in the North Atlantic at 2000–2400 m (Figure 6, G5). The low amplitude of the $\delta^{18}O_{b\text{-}ivc}$ curves compared with the G1 cores point to a southward flow of BSW-induced intermediate water from the Nordic seas into the North Atlantic at 2000–2400 m. This is in agreement with *Waelbroeck et al.* [2006].

[31] Below 2400 m in the North Atlantic, decreasing $\delta^{18}O_{b\text{-}ivc}$ values through the ED do not directly correspond with decreasing $\delta^{13}C_b$ values (Figure 6, G5). Thus they could potentially reflect warming of deep water. However, $\delta^{13}C_b$ values were still low compared to the Holocene, and we instead suggest that elevated $\delta^{13}C_b$ values toward the end of the ED could originate from brine-influenced intermediate water from the Nordic seas, with higher ^{13}C values than the ^{13}C poor SOW. SOW may thus have no large

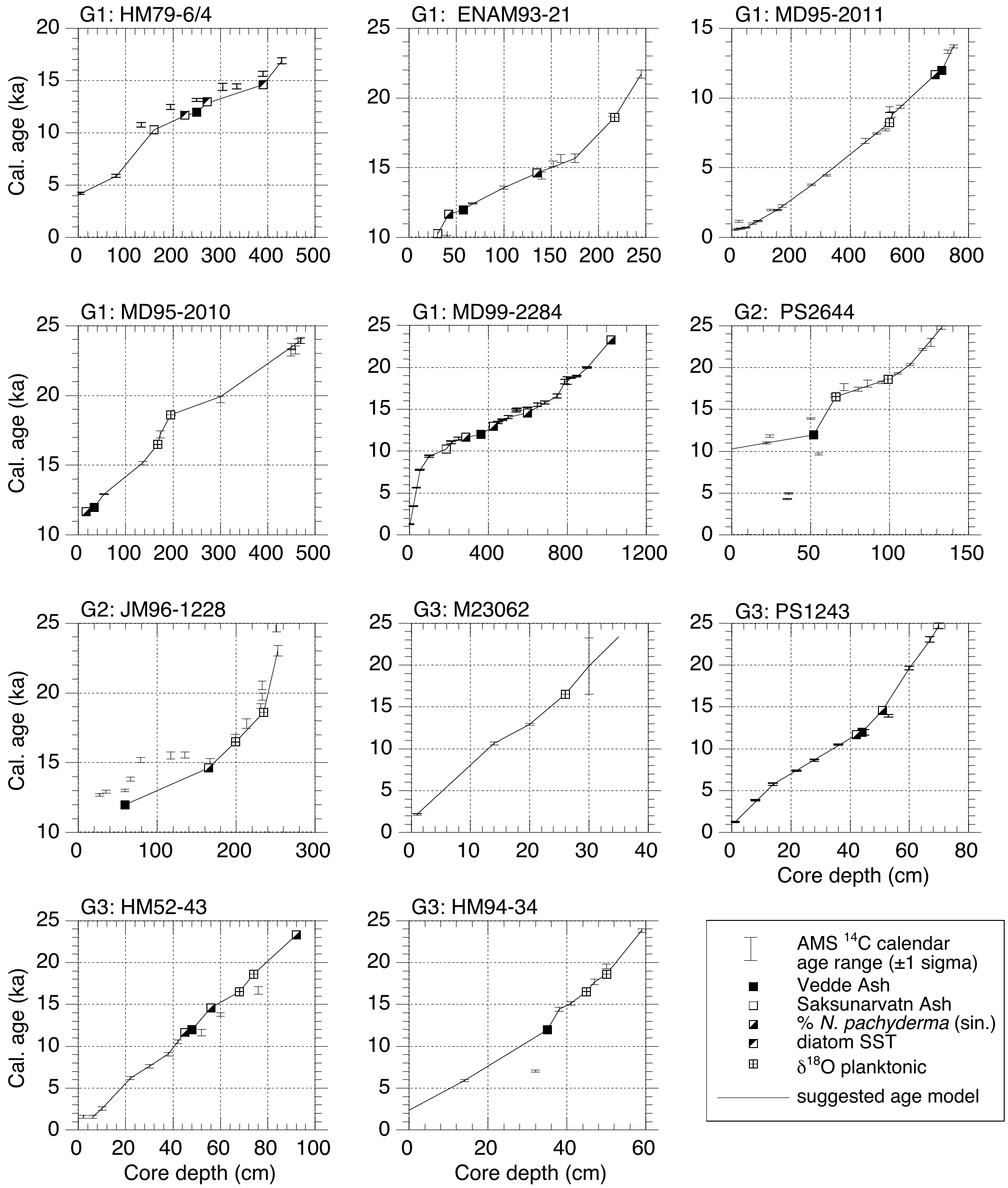

Figure 4. Age models for all cores reconstructed in this study. The numbers G1–G5 refer to the group definition described in section 2.1 and Table 1. The age of the correlation points shown in the age models (percent *N. pachyderma* (s), SST, and $\delta^{18}O_{planktonic}$) are found directly from the NGRIP ice core ages shown in Tables 2a and 2b. he suggested age models are reconstructed from a combination of the correlation points and the AMS ^{14}C dates, where the correlation points are suggested to be more precise time markers than the AMS ^{14}C dates.

influence at depths below 2000 m in the North Atlantic. Instead, we suggest that brine-enriched intermediate water formed in the Nordic seas did entrain waters also below 2500 m in the North Atlantic in a significant way.

3.4. Bølling-Allerød (14.7–12.9 ka)

[32] From the ED into the BA $\delta^{18}O_{b\text{-}ivc}$ values increased with 1–2‰ on intermediate depths in the eastern Nordic seas, and reached approximately modern values (Figures 6 and 8d, G1). This increase suggests a cease of large meltwater events and brine formation along the European margin. Warmer climate also gave worsened conditions for potential large-scale BSW formation in the shallow North Sea. Modern ocean conditions were recovered at intermediate depths. A $\delta^{18}O_{b\text{-}ivc}$ increase into the BA and $\delta^{13}C_b$ values higher than modern (Figure 6, G4) are also observed in the North Atlantic core BOFS17K. This increase indi-

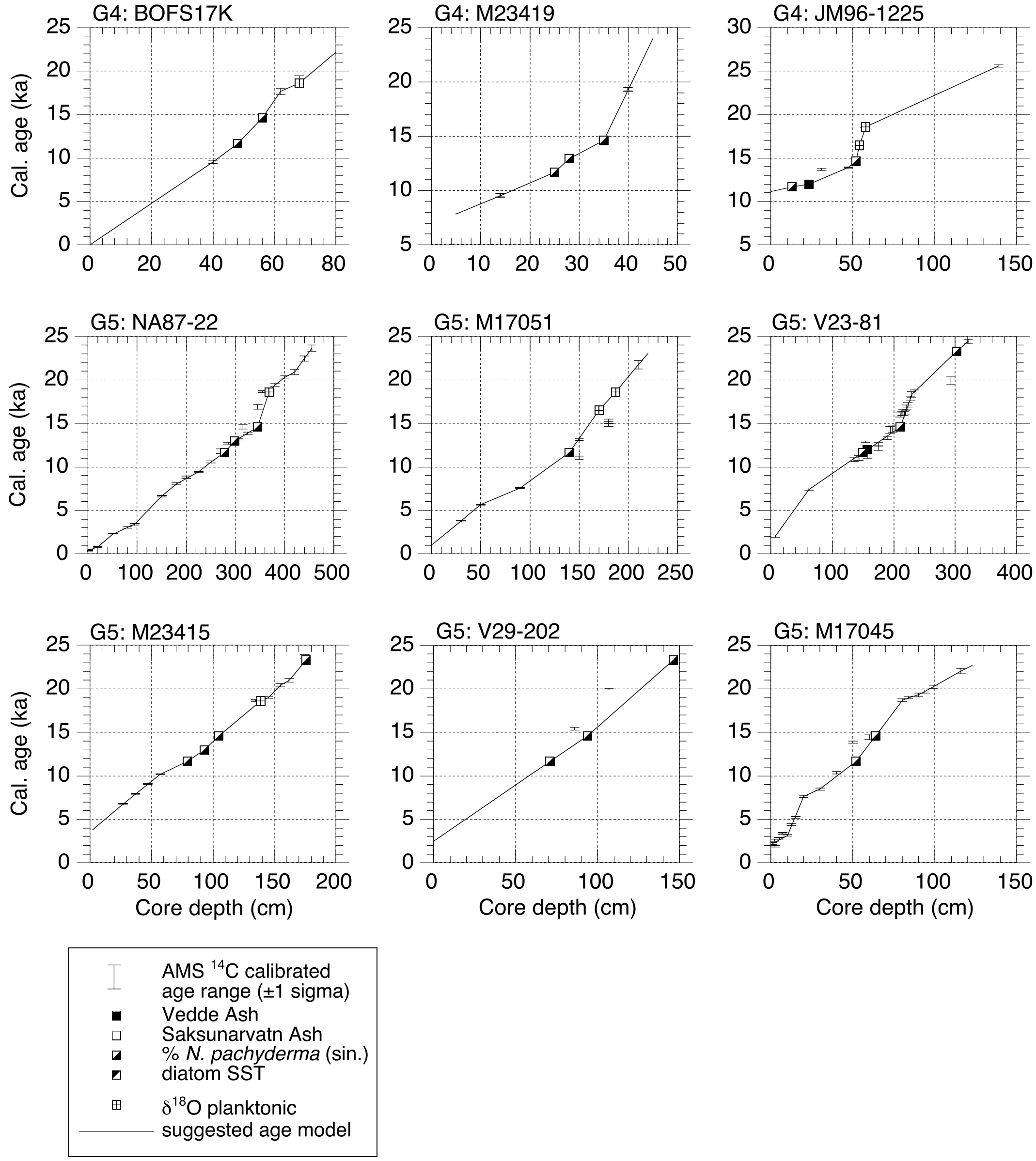

Figure 4. (continued)

cates an intermediate water mass here influenced by a cold water mass convected in an open ocean. We suggest that intermediate water formed in the Nordic seas flowed through the Iceland-Scotland Ridge, and were able to influence depths down to at least 1150 m.

[33] On intermediate depths in the western Nordic seas, a $\delta^{18}O_{b\text{-ivc}}$ increase is also observed, but the values had large and rapid fluctuations. A positive correlation between $\delta^{18}O_{b\text{-ivc}}$ and $\delta^{13}C_b$ changes (Figure 6, JM96-1228 in G2) indicates rapid changes between brine-influenced and convective bottom water during this period. A similar tendency is also observed west of Iceland (Figure 6, JM96-1225 in G4). Since the largest isotope changes are observed in JM96-1228, we suggest that brine-enriched bottom water in periods flowed from the Nordic seas to the North Atlantic via the Denmark Strait. Lower $\delta^{18}O_p$ values in G2 cores than in G1 cores (Figure 5) imply that ^{18}O-poor meltwaters from the Greenland and/or Iceland ice caps were more visible in both the planktonic and benthic oxygen isotopes than further east. Thus open-ocean convection and meridional overturning during the BA was probably easterly located compared to the Holocene, and was not able to sufficiently dilute meltwater and brine water signals in the western Nordic seas.

[34] A marked increase in $\delta^{18}O_{b\text{-ivc}}$ is noted below 2000 m in the Nordic seas, combined with slightly increased $\delta^{13}C_b$ values (Figure 6, G3). We suggest that this combination reflects a larger degree of open-ocean convection in the Nordic seas. Still $\delta^{18}O_{b\text{-ivc}}$ and $\delta^{13}C_b$ values were lower than modern values (Figure 6, G3), suggesting a brine

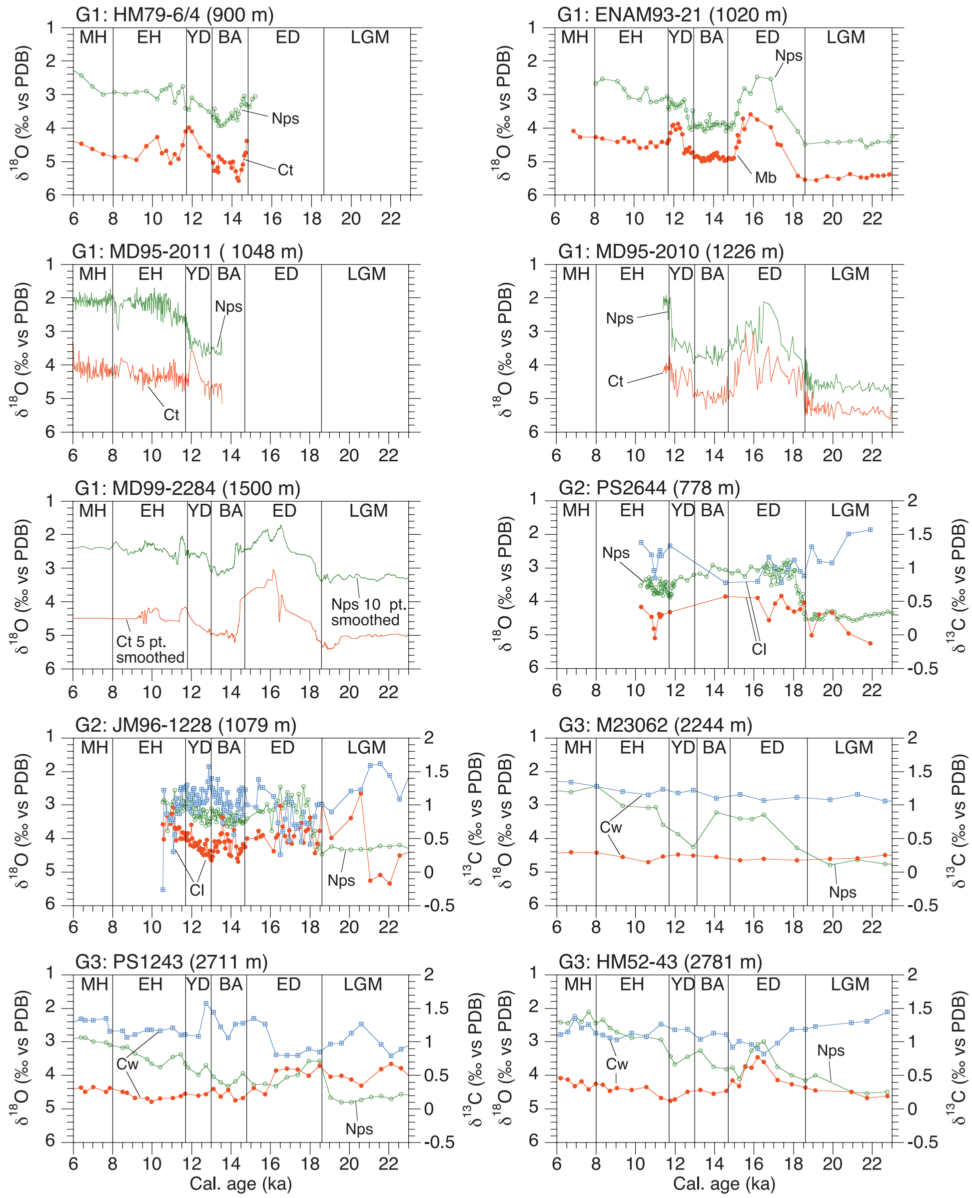

Figure 5. The δ^{18}O records of planktonic (green curves) and benthic foraminifera (red curves) and $\delta^{13}C_b$ records of epibenthic foraminifera (blue curves) from the cores shown in Figure 1. The calibrated age scales are deduced from the core depths using the age models in Figure 4. The vertical lines denote the boundaries between the different time intervals. The headers (groups 1–5) denote the "group affiliation" of the different cores, with reference to section 2.1 and Table 1. Abbreviations are Nps, *N. pachyderma* (s); Gb, *G. bulloides*; Ct, *C. teretis*; Cw, *C. wuellerstorfi*; Cl, *C. lobatulus*; Mb, *M. barleeanum*; and Ou, *O. umbonatus*. For information about "Modern" benthic isotope values (0–6 ka), see Figure 8.

signal, possibly from the same source as the intermediate water mass in the western Nordic seas.

[35] In the North Atlantic, at depths somewhere below 1150 m, $\delta^{18}O_{b\text{-ivc}}$ values decreased on average from the ED to the BA (Figures 6, 8d, and 8i, G4 and G5). We suggest that this decrease was at least partly caused by a warming of deep water in the North Atlantic, because of a larger influence of NADW. Benthic foraminiferal Mg/Ca data suggest North Atlantic deepwater temperatures of 2°–2.5°C at 3100 m depth on the Iberian Margin [*Skinner et al.*, 2003], almost as high as today. An overall $\delta^{13}C_b$ increase is observed in cores below 2000 m (Figure 6, G5), and supports this suggestion. Compared to the Holocene average $\delta^{13}C_b$ values in G5 cores were significantly lower. The $\delta^{13}C_b$ difference between the BA and the Holocene is not so obvious in most of the G2, G3, and G4 cores. We propose that NADW with modern characteristics entrained depths below 2000 m in the North Atlantic,

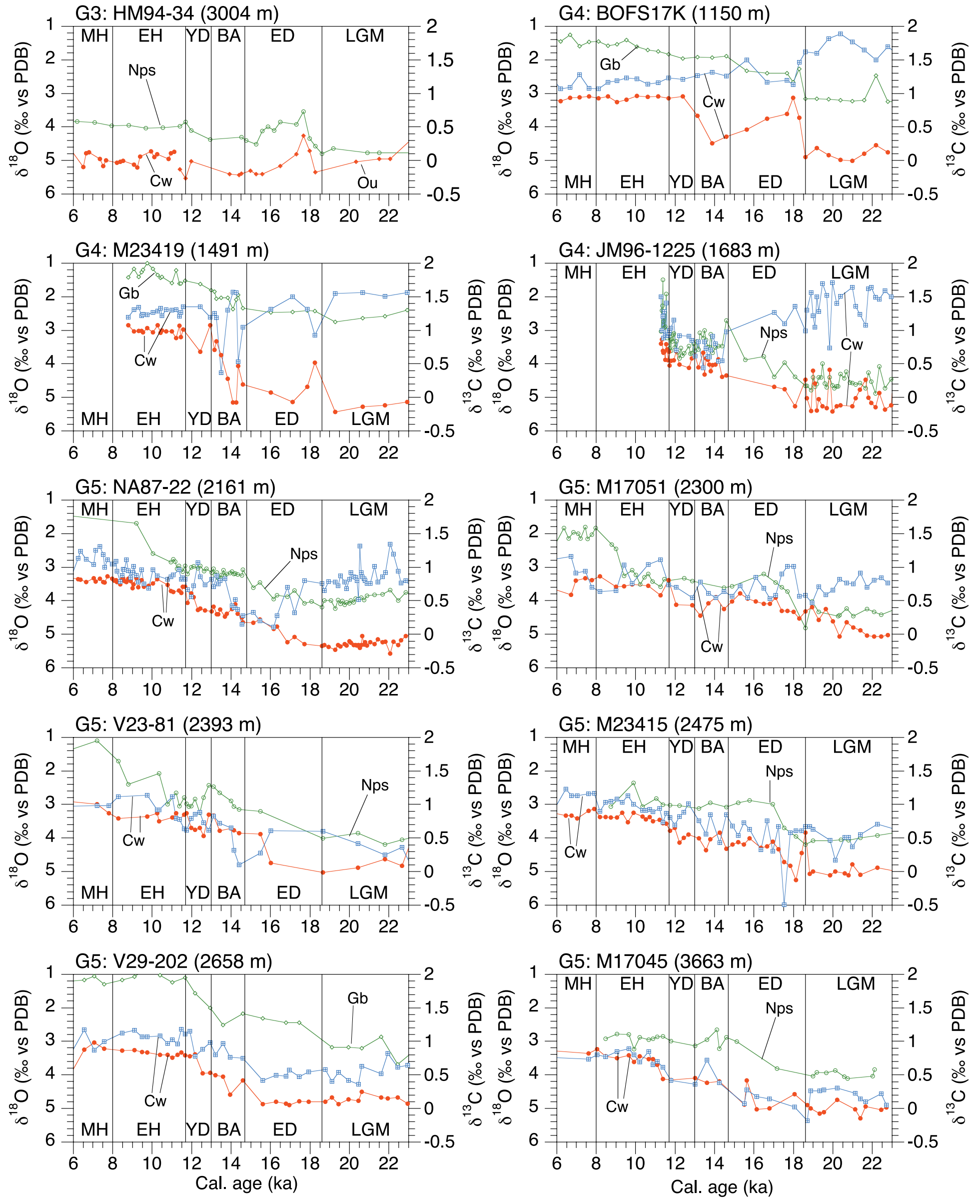

Figure 5. (continued)

but not in similar amounts as during the Holocene. This finding is confirmed by recent ^{231}Pa/^{230}Th data [*Gherardi*, 2006]. SOW or BSW-enriched waters probably occupied water masses below 2000 m to a higher degree than today. A large meltwater pulse from the Antarctica at ~14 ka [*Kanfoush et al.*, 2000] may have caused enhanced brine formation there and promoted transport of brine-enriched SOW at depths below 2000 m into the North Atlantic. Parts of the low $\delta^{18}O_{b\text{-ivc}}$ and $\delta^{13}C_b$ signals were therefore probably due to BSW-enriched SOW.

3.5. Younger Dryas (12.9–11.7 ka)

[36] A decrease in $\delta^{18}O_{b\text{-ivc}}$ at intermediate depths in the Nordic seas (Figures 6, 8e, and 8j, G1 and G2) suggests brine formation. Low-δ^{18}O meltwater sank to intermediate depths in the southeastern Nordic seas, but not to the same extent as during the ED, since the $\delta^{18}O_{b\text{-ivc}}$ amplitude was smaller for the YD (Figure 6, G1). Shallow areas potentially covered a larger area compared to the ED, because of global sea level increase [*Fairbanks*, 1989; *Lambeck and Chappell*, 2001] and lower glacial ice volume [*Peltier*, 1994]. Thus BSW formation may have been at least as intensive as during the ED. However, since glacial melting was not as intensive as during the ED, the potential for making large $\delta^{18}O_{b\text{-ivc}}$ depletions to intermediate and deep waters were not that good.

[37] Brine-enriched water in the Nordic seas probably did not sink below 2000 m in large amounts, thereby explaining higher $\delta^{18}O_{b\text{-ivc}}$ and $\delta^{13}C_b$ values found in the G3 cores (Figure 6). High $\delta^{13}C_p$ values [*Sarnthein et al.*, 1995] and high $\delta^{13}C_b$ values (Figure 6, G3) indicate some open-ocean

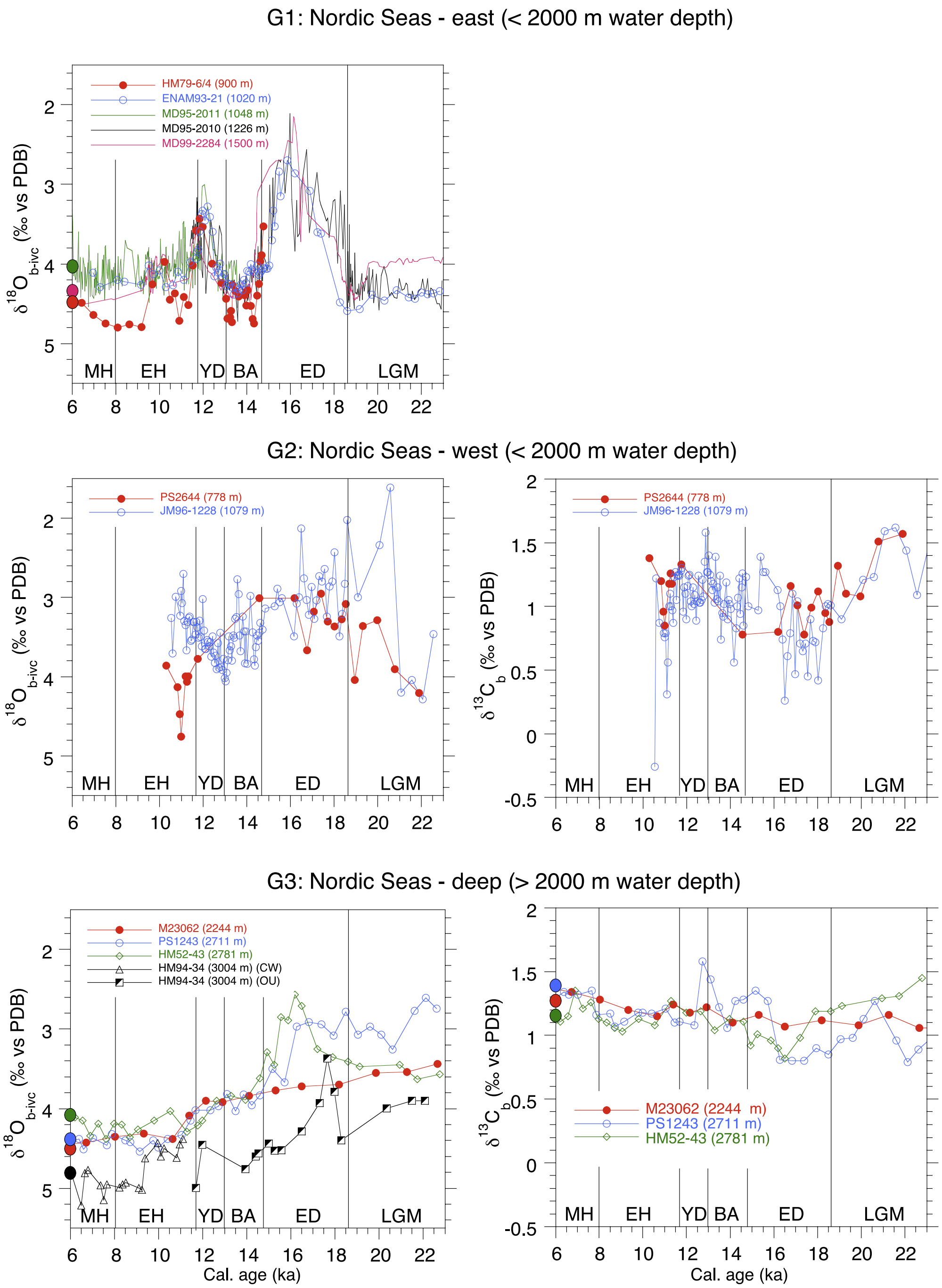

Figure 6. Ice volume–corrected (left) benthic oxygen and (right) benthic carbon isotope records (approach described in section 2.3). The records are grouped based on the group definition described in section 2.1 and Table 1. See section 2.4 for details about the time interval abbreviations. The average values of the "Modern" benthic isotope values (0–6 ka) are marked as circles on the left *y* axes (see also Figure 8). These circles are marked only for cores with at least three benthic isotope values for the period 0–6 ka. The color of each circle refers to the color code for each core. Owing to the lack of deglacial and glacial epibenthic $\delta^{13}C_b$ records in the G1 cores and HM94-34, these records are not shown here.

convection in the Nordic seas. On the basis of our data, layering of water masses was nearly opposite to the LGM, with more brine-enriched water above 2000 m and more open-ocean convected water below 2000 m in the Nordic seas. Cold winters probably abetted the sinking of BSW, and some open-ocean convection with surface cooling influenced deepwater formation in the Nordic seas. In combination these factors may have caused relatively high $\delta^{18}O_{b\text{-ivc}}$ and $\delta^{13}C_b$ values in deep water (Figure 6, G3) and

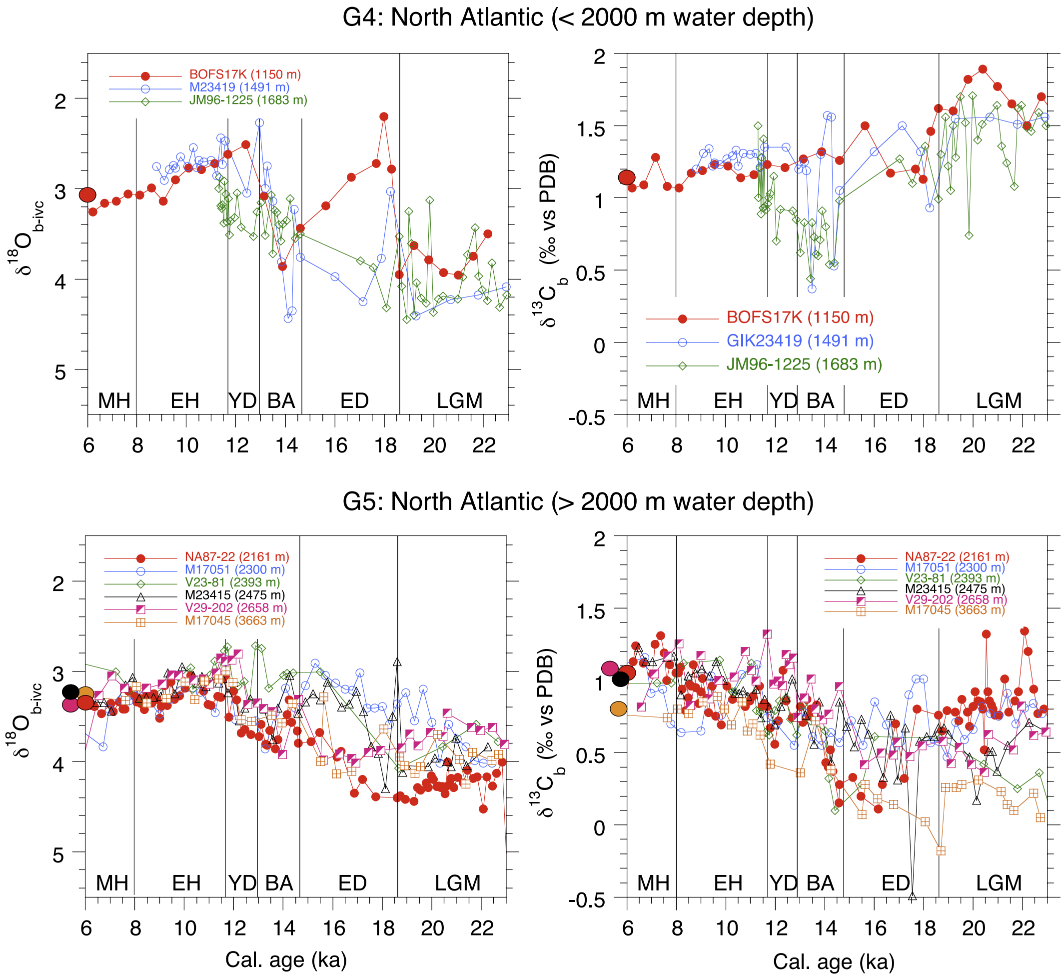

Figure 6. (continued)

lowered $\delta^{18}O_{b\text{-ivc}}$ values in intermediate water (Figure 6, G1).

[38] In the North Atlantic $\delta^{18}O_{b\text{-ivc}}$ and $\delta^{13}C_b$ values decreased and increased, respectively, from the BA into the YD (Figure 6, G4 and G5). This combination could indicate a transition to warmer and well-ventilated water masses. However, south of 40°N, below 3000 m depth, benthic $\delta^{13}C_b$ values [*Boyle and Keigwin*, 1987; *Labeyrie et al.*, 2005; *Skinner and Shackleton*, 2005] and sediment $^{231}Pa/^{230}Th$ ratios [*McManus et al.*, 2004; *Gherardi et al.*, 2005] indicate a reduced NADW flow compared to the Bølling-Allerød and the Holocene. Combined benthic Mg/Ca ratios and oxygen isotope measurements suggest a deepwater cooling of 2°–3°C and a $\delta^{18}O_{deepwater}$ lowering of ~1‰ from the BA into the YD on ~3100 m depth at the Iberian Margin [*Skinner et al.*, 2003]. *Keigwin* [2004] also suggests young ventilation ages above 2300 m in the western subtropical North Atlantic during the YD, and older ages below 2300 m. He concludes that the LGM and YD modes of ocean circulation were the same. Depths above 1500 m seem to be better ventilated than below, based on $\delta^{13}C_b$ records in the North Atlantic (Figure 6, G4 and G5). Thus we support the conclusion of *Keigwin* [2004], but suggest a shallower boundary between well and poorly ventilated water.

[39] If we assume deepwater cooling of ~2°C from the BA into the YD for our North Atlantic cores, in accordance with the Iberian Margin [*Skinner et al.*, 2003], $\delta^{18}O_{deepwater}$ must have been lowered by at least ~0.5‰ to explain a slight lowering of $\delta^{18}O_{b\text{-ivc}}$. Taken in fact a lowering of about ~1‰ from the BA to the YD at intermediate depths in the Nordic seas (Figure 6, G1 and G2), we suggest that BSW-enriched water flowed from the Nordic seas and mixed with waters below ~1500 m in the North Atlantic. A slight BA-YD increase in $\delta^{13}C_b$ in the brine-influenced North Atlantic deep water (Figure 6, G4 and G5) may at first seem as a paradox. However, we have an explanation: brine-enriched intermediate water in the Nordic seas may have contained some ^{13}C-enriched water made from open-ocean convection, or contained debris slightly enriched in ^{13}C. When this water mass entrained deep water in the North Atlantic, it more or less replaced deep water formed during Bølling-Allerød, which had relatively low $\delta^{13}C_b$ values because of some influence of brine/SOW (see section 3.4).

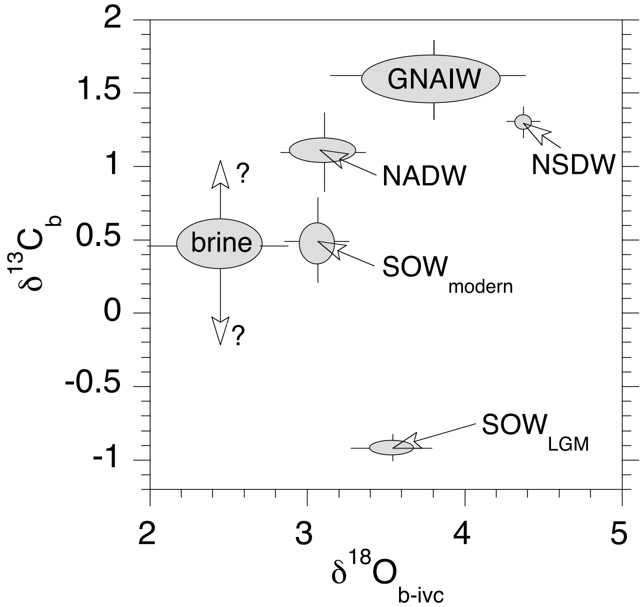

Figure 7. Typical $\delta^{18}O_{b\text{-ivc}}$ and $\delta^{13}C_b$ values for epibenthic foraminifera with respect to different water masses. The horizontal and vertical lines mark the approximate ranges for each of the water masses. The $\delta^{18}O_{b\text{-ivc}}$ values are corrected for +0.64‰ [*Graham et al.*, 1981; *Jansen et al.*, 1988]. Abbreviations are GNAIW, Glacial North Atlantic Intermediate Water; NADW, North Atlantic Deep Water; NSDW, Norwegian Sea Deep Water; SOW, Southern Ocean Water; and LGM, Last Glacial Maximum. The water masses NADW, NSDW, and SOW_{modern} represent modern conditions, while the other water masses represent isotope ranges of glacial conditions, interpreted by *Vogelsang* [1990], *Dokken and Jansen* [1999], *Hagen and Hald* [2002], *Curry and Oppo* [2005], and this work. The question marks mean that the $\delta^{13}C_b$ ranges for brine-enriched water is not well known yet.

3.6. Early Holocene and Mid-Holocene (11.7–6 ka)

[40] A transition to generally higher and "modern-like" $\delta^{18}O_{b\text{-ivc}}$ and $\delta^{13}C_b$ values at the YD-EH transition occurred in both the Nordic seas and the North Atlantic (Figures 6, 8f, and 8k). We suggest that intermediate and deep water became less influenced by brine rejection during the EH, because of reduced BSW formation due to warmer climate. The Nordic seas deepwater properties seemed to resemble modern conditions. Still, cold conditions and BSW formation potentially at the Greenland and/or Iceland shelves (Figure 9) seems to have yielded brine-enriched water to depths of 1000–1100 m. Decreased $\delta^{18}O_{b\text{-ivc}}$ and $\delta^{13}C_b$ values at ~11.0 ka suggest this (Figure 6, G2). The same is observed at similar depths at the Vøring Plateau (MD95-2011). Glacial melting and still cold conditions may have favored BSW formation landward of the Vøring Plateau, but in smaller scale compared to the ED and the YD.

[41] Around 11–9 ka, a return to lower $\delta^{18}O_{b\text{-ivc}}$ values is observed mainly in the three cores in the southeastern Nordic seas (Figure 6, G1). This decrease is paralleled by SST coolings [*Karpuz and Jansen*, 1992; *Hald and Hagen*, 1998; *Andersen et al.*, 2004] and low $\delta^{18}O_p$ events (potential meltwater events, see Figure 5), which could enhance brine formation. One or more large meltwater events may have contributed to this $\delta^{18}O_{b\text{-ivc}}$ decrease. A locality close to the Fennoscandian ice sheet, including drainage of large ice-dammed lakes in eastern Norway at that time [*Liestøl*, 1956], is a potential cause for meltwater events with following brine formation.

[42] Low $\delta^{18}O_{b\text{-ivc}}$ events (combined with low $\delta^{13}C_b$) are not seen in the North Atlantic, suggesting that local melting episodes in the Nordic seas do not contribute significantly to water masses in the North Atlantic. After this event a $\delta^{18}O_{b\text{-ivc}}$ increase into the MH in the Nordic seas cores and partly in the North Atlantic (Figures 6, 8g, and 8l) is observed. The $\delta^{18}O_{b\text{-ivc}}$ values were also generally higher than during the last 6 ka in the Nordic seas, while they were more or less similar to modern in the North Atlantic. The MH is a period also called "the Holocene warm optimum" and is well documented by warmer sea surface [*Koç et al.*, 1993; *Andersen et al.*, 2004] and disappearance of Norwegian ice caps [*Nesje and Dahl*, 1993]. During this warm period high $\delta^{18}O_{b\text{-ivc}}$ values may have been caused by decreased brine influence from the Storfjorden area (at Svalbard) and from Siberian margins, which occurs today [*Quadfasel et al.*, 1988; *Martin and Cavalieri*, 1989; *Fer et al.*, 2003; *Skogseth et al.*, 2005].

[43] The 8.2 ka cold event, found in the $\delta^{18}O$ record from the Greenland ice cores [*Grootes et al.*, 1993; *Stuiver et al.*, 1995; *Rasmussen et al.*, 2006], does not stand out in our isotope records, except at the Vøring plateau (Figure 6, MD95-2011) [*Risebrobakken et al.*, 2003]. This is possibly due to low early Holocene resolution in the other cores.

4. Summary and Conclusions

[44] This study has synthesized previously published and new benthic oxygen isotope data from the Nordic seas and the northern North Atlantic. Benthic carbon isotope and planktonic oxygen isotope data are used to support our interpretations. The study updates previous investigations, and demonstrates how changes in intermediate and deep-water masses influenced ocean circulation in a larger geographical and vertical coverage compared to previous studies.

[45] During the LGM a well-ventilated intermediate water mass in the Nordic seas was formed and layered at depths above 1500 m. It crossed the Iceland-Scotland Ridge and entrained waters in the North Atlantic above 2000 m, as suggested by high $\delta^{13}C_b$ values in the G4 cores. This water mass also partly entrained waters down to at least ~3700 m, suggesting that SOW did not penetrate as shallow and far north as previously suggested in several studies. The well-ventilated water mass in the Nordic seas was probably not dense enough to sink further down in large amounts here. Instead, brine-enriched water occupied water depths below 1500 m in the Nordic seas.

[46] During the ED intensive brine formation lead to large-scale sinking of $\delta^{18}O$-depleted meltwater to intermediate depths in the Nordic seas. BSW-enriched waters also

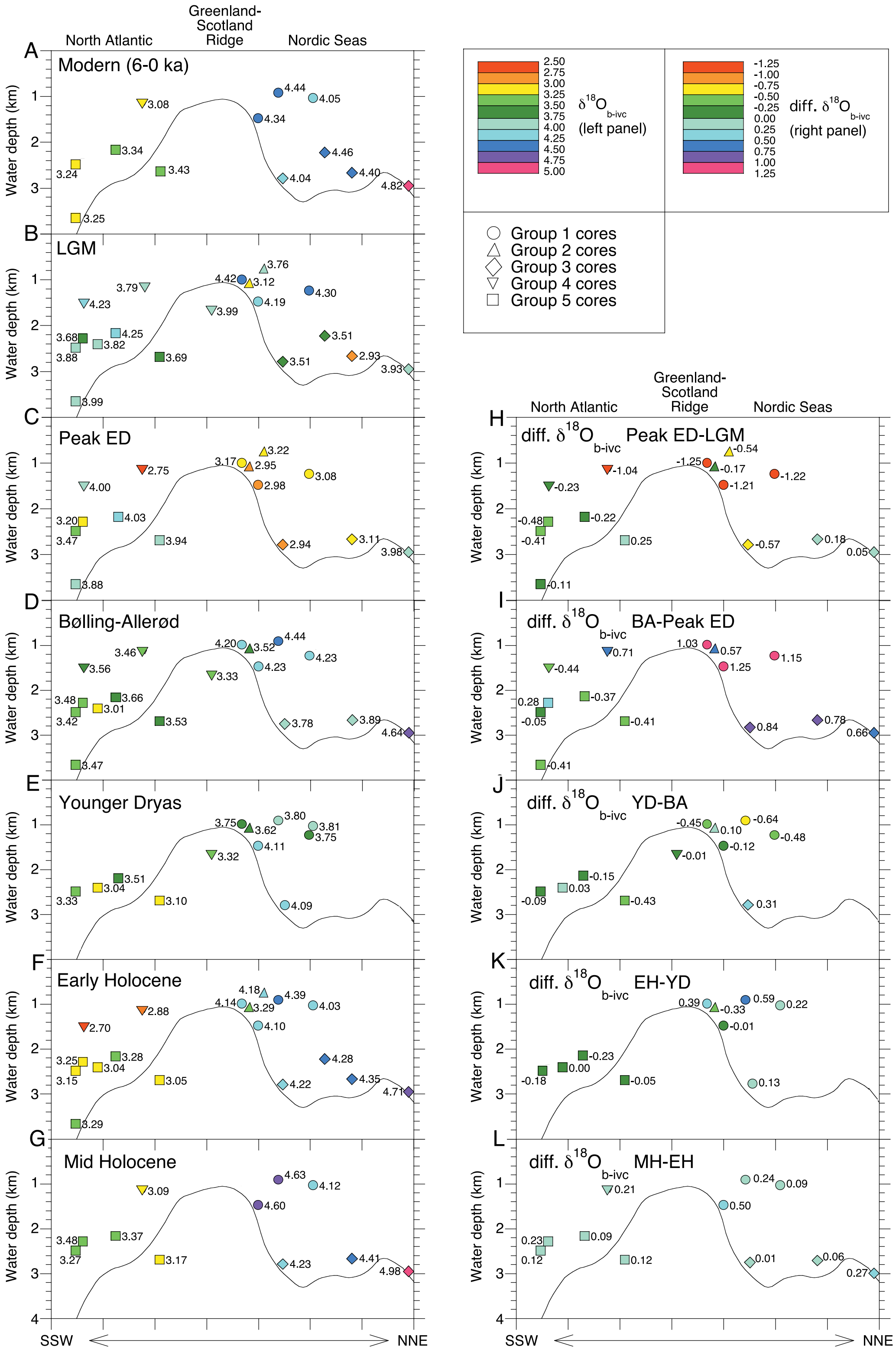

Figure 8. (a–g) Benthic $\delta^{18}O_{b\text{-}ivc}$ profiles for seven different time slices. Vertical plots show bathymetry, water masses, current flows, and average $\delta^{18}O_{b\text{-}ivc}$ values (averages of measurements from at least three different core depth levels in each time slice). (h–l) Difference in $\delta^{18}O_{b\text{-}ivc}$ between the different time slices. "Peak ED" is defined as the period 18.0–15.5 ka B.P., in which the lowest $\delta^{18}O_{b\text{-}ivc}$ values for the ED are observed in our cores.

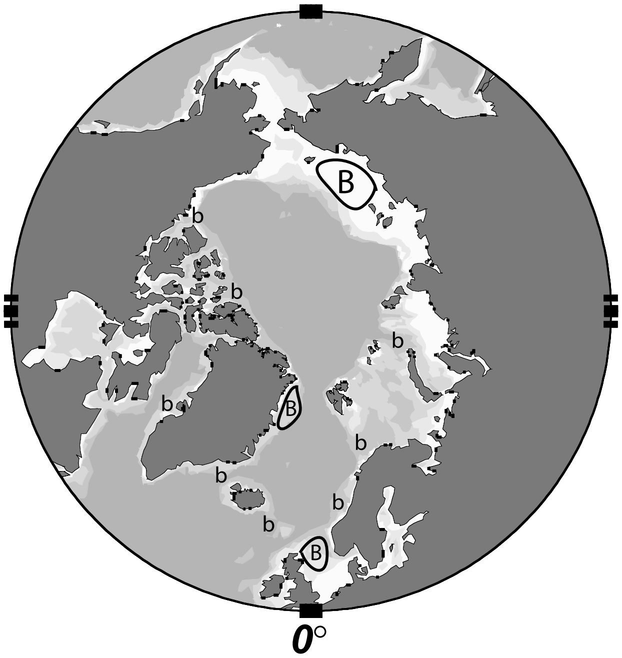

Figure 9. Map of the Northern Hemisphere. The areas marked with "B" and constrained by black borders show potential areas where large-scale brine formation hypothetically may have occurred, explaining the low $\delta^{18}O_{b\text{-}ivc}$ excursions in cold periods. Common for these areas are that they were large and shallow deglaciated shelf areas with water depths of less than 200 m at ~17 ka [*Peltier*, 1994]. The areas marked "b" were also potential areas of brine formation, but because of smaller areas and larger water depths (200–500 m at ~17 ka) the potential for making large undiluted volumes of $\delta^{18}O_w$-depleted water was lower.

periodically influenced depths below 2000 m there. The most intensive period of brine formation was during 17–15 ka, where it was most pronounced in the eastern Nordic seas intermediate water masses. This water mass flowed southward, crossing the Greenland-Scotland Ridge, and extended southward into the North Atlantic. There, water depths above 2200 m were intruded by significant amounts of this brine-enriched water mass. Also water depths below 2200 m were influenced by these brine-enriched water masses from the Nordic seas.

[47] During the BA open-ocean convection and meridional overturning in the Nordic seas indicate that the AMOC strengthened, however, not to the same strength as today. Convected water entrained shallower depths than today, but contained similar properties as today at intermediate depths, reflected in the benthic foraminiferal isotopes. This water outflowed southward across the Iceland-Scotland Ridge. In the Denmark Strait there also was outflow, but here the water masses experienced rapid and intermittent changes between well-ventilated and brine-enriched water compared with today. The NADW with modern characteristics did not entrain depths below 2000 m in the North Atlantic in similar amounts as during the Holocene.

[48] Colder conditions during the YD lead to an increase in sea ice freezing and sinking of BSW to intermediate depths in the Nordic seas. However, at least some open-ocean convection and meridional overturning probably existed there. The water mass resulting from this convection mixed with BSW during the cold winter season, though not as intensive as during the ED, since glacial melting was less intensive. The mixed intermediate water mass flowed southward and crossed the Greenland-Scotland Ridge. Depths above 1500 m in the North Atlantic were clearly influenced by a well-ventilated water mass outflow from the Nordic seas, with contribution from both open-ocean convection and brine. Also water depths from 1500 m and down to 3700 m depth were influenced by outflow from the Nordic seas.

[49] At the entrance to the Holocene there was a transition to more and deeper lying well-ventilated water in both the Nordic seas and the North Atlantic. NADW flow became vigorous down to depths of at least ~3700 m. Lowered $\delta^{18}O_{b\text{-}ivc}$ values at intermediate depths in the eastern Nordic seas indicate a meltwater event around ~10 ka. The origin is unknown, but we suggest that the best potential candidate is meltwater from the waning Fennoscandian ice sheet, possibly including draining of large ice-dammed lakes in Norway. During the period 8–6 ka (MH), the $\delta^{18}O_{b\text{-}ivc}$ values were also higher than today, indicating warmer conditions and less brine formation from Storfjorden at Svalbard, compared with today.

[50] Our conclusion that the marked $\delta^{18}O_{b\text{-}ivc}$ depletions in the Nordic seas mainly were caused by brine-enriched meltwater seems fairly robust, since there potentially were favorable conditions in shallow seas, like the North Sea, outside the northeastern Greenland and the Arctic Ocean margin north of east Siberia. However, we see that more work, including geochemical and modeling investigations, should be performed to get a more robust interpretation of the $\delta^{18}O_{b\text{-}ivc}$ depletions as reflecting brine-enriched bottom water. Other geochemical proxies, for instance benthic foraminiferal Mg/Ca ratios, may constrain the temperature component with larger confidence. Other geochemical proxies like $^{231}Pa/^{230}Th$ in the sediment and Cd/Ca of benthic foraminifera, may also aim interpretation of bottom water properties and constrain flow dynamics of the AMOC.

[51] Intermediate and deep water was generated more or less continuously in the Nordic seas during 23–6 ka, but with different proportions of brine and open-ocean convected water. Even if BSW was produced during the LGM and the YD cold periods, there were still open-ocean convection and meridional overturning. This study supports previous work in the way that cold conditions and weak Atlantic meridional overturning are not always paralleled.

[52] **Acknowledgments.** This manuscript was greatly improved by detailed and constructive reviews from two anonymous reviewers and Gerald Dickens. Comments and suggestions from Claire Waelbroeck, Ulysses Silas Ninnemann, and Carin Andersson Dahl also clearly improved the manuscript. Cathy Jenks corrected the English grammar and language. Rune Søraas and Odd Hansen are thanked for keeping the stable isotope mass spectrometer in good shape. The project is funded by the Bjerknes Centre for Climate Research and by the Norwegian Research Foundation (NFR) through two RAPID projects: ORMEN: The impact of changing freshwater flows on the thermohaline circulation and European climate and VAMOC: Variability of the Atlantic Meridional Overturning Circulation. This is publication A178 from the Bjerknes Centre.

References

Andersen, C., N. Koç, and M. Moros (2004), A highly unstable Holocene climate in the subpolar North Atlantic: Evidence from diatoms, *Quat. Sci. Rev.*, *23*, 2155–2166.

Atkinson, T. C., K. R. Briffa, and G. R. Coope (1987), Seasonal temperatures in Britain during the past 22,000 years reconstructed using beetle remains, *Nature*, *325*, 587–592.

Bard, E., B. Hamelin, M. Arnold, L. Montaggioni, G. Cabioch, G. Faure, and F. Rougerie (1996), Deglacial sea-level record from Tahiti corals and the timing of global meltwater discharge, *Nature*, *382*, 241–244.

Bauch, H. A., H. Erlenkeuser, R. F. Spielhagen, U. Struck, J. Matthiessen, J. Thiede, and J. Heinemeier (2001), A multiproxy reconstruction of the evolution of deep and surface water in the subarctic Nordic seas over the last 30,000 yr, *Quat. Sci. Rev.*, *20*, 659–678.

Björck, S., et al. (1996), Synchronized terrestrial/atmospheric deglacial records around the North Atlantic, *Science*, *274*, 1155–1160.

Bond, G., W. Broecker, S. Johnsen, J. McManus, L. Labeyrie, J. Jouzel, and G. Bonani (1993), Correlations between climate records from North Atlantic sediments and Greenland ice, *Nature*, *365*, 143–147.

Bondevik, S., J. Mangerud, H. H. Birks, S. Gulliksen, and P. J. Reimer (2006), Changes in North Atlantic radiocarbon reservoir ages during the Allerød and Younger Dryas, *Science*, *312*, 1514–1517.

Boyle, E. A., and L. Keigwin (1987), North Atlantic thermohaline circulation during the last 20,000 years: Link to high latitude surface temperature, *Nature*, *330*, 35–40.

Broecker, W. S., M. Andree, W. Wolfli, H. Oeschger, G. Bonani, J. Kennett, and D. Peteet (1988), The chronology of the last deglaciation: Implications to the cause of the Younger Dryas event, *Paleoceanography*, *3*, 1–19.

Curry, W. B., and D. W. Oppo (2005), Glacial water mass geometry and the distribution of $\delta^{13}C$ of ΣCO_2 in the western Atlantic Ocean, *Paleoceanography*, *20*, PA1017, doi:10.1029/2004PA001021.

Dokken, T., and E. Jansen (1999), Rapid changes in the mechanism of ocean convection during the last glacial period, *Nature*, *401*, 458–461.

Drange, H., T. Dokken, T. Furevik, R. Gerdes, W. Berger, A. Nesje, K. A. Orvik, Ø. Skagseth, I. Skjelvan, and S. Østerhus (2005), The Nordic seas: An overview, in *The Nordic Seas: An Integrated Perspective*, *Geophys. Monogr. Ser.*, vol. 158, edited by H. Drange et al., pp. 1–10, AGU, Washington, D. C.

Duplessy, J.-C., N. J. Shackleton, R. K. Matthews, W. Prell, W. F. Ruddiman, M. Caralp, and C. H. Hendy (1984), $\delta^{13}C$ record of benthic foraminifera in the last interglacial ocean: Implications for the carbon cycle and the global deep water circulation, *Quat. Res.*, *21*, 225–243.

Duplessy, J.-C., N. J. Shackleton, R. G. Fairbanks, L. Labeyrie, D. Oppo, and N. Kallel (1988), Deep water source variations during the last climatic cycle and their impact on the global deepwater circulation, *Paleoceanography*, *3*, 343–360.

Duplessy, J.-C., L. Labeyrie, M. Arnold, M. Paterne, J. Duprat, and T. C. E. van Weering (1992), Changes in surface salinity of the North Atlantic during the last deglaciation, *Nature*, *358*, 485–488.

Duplessy, J.-C., L. Labeyrie, and C. Waelbroeck (2002), Constraints on the ocean oxygen isotopic enrichment between the Last Glacial Maximum and the Holocene: Paleoceanographic implications, *Quat. Sci. Rev.*, *21*, 315–330.

Fairbanks, R. G. (1989), A 17,000-year glacio-eustatic sea level record: Influence of glacial melting rates on the Younger Dryas event and deep-ocean circulation, *Nature*, *342*, 637–642.

Fer, I., R. Skogseth, P. M. Haugan, and P. Jaccard (2003), Observations of the Storfjorden overflow, *Deep Sea Res., Part I*, *50*, 1283–1303.

Gherardi, J.-M. (2006), Changements de la Circulation Océanique au cours de la Déglaciation: Apport des traceurs $^{231}Pa/^{230}Th$ du sédiment et Mg/Ca des foraminiféres benthiques, Ph.D. thesis, Lab. des Sci. du Clim. et de L'environ., Univ. Pierre and Marie Curie, Paris.

Gherardi, J.-M., L. Labeyrie, J. F. McManus, R. Francois, L. C. Skinner, and E. Cortijo (2005), Evidence from the northeastern Atlantic basin for variability in the rate of the meridional overturning circulation through the last deglaciation, *Earth Planet. Sci. Lett.*, *240*, 710–723.

Graham, D. W., B. H. Corliss, M. L. Bender, and L. D. Keigwin (1981), Carbon and oxygen disequilibria of recent deep-sea benthic foraminifera, *Mar. Micropaleontol.*, *6*, 483–497.

Grönvold, K., N. Óskarsson, S. J. Johnsen, H. B. Clausen, C. U. Hammer, G. Bond, and E. Bard (1995), Ash layers from Iceland in the Greenland GRIP ice core correlated with oceanic and land sediments, *Earth Planet. Sci. Lett.*, *135*, 149–155.

Grootes, P., M. Stuiver, J. W. C. White, S. Johnsen, and J. Jouzel (1993), Comparison of oxygen isotope records from the GISP2 and Greenland ice cores, *Nature*, *366*, 552–554.

Hagen, S. (1999), North Atlantic paleoceanography and climate history during the last 70 cal. ka, Dr. Sci. thesis, Univ. of Bergen, Bergen, Norway.

Hagen, S., and M. Hald (2002), Variation in surface and deep water circulation in the Denmark Strait, North Atlantic, during marine isotope stages 3 and 2, *Paleoceanography*, *17*(4), 1061, doi:10.1029/2001PA000632.

Hald, M., and S. Hagen (1998), Early Preboreal cooling in the Nordic seas region triggered by meltwater, *Geology*, *26*, 615–618.

Hansen, B., S. Østerhus, D. Quadfasel, and B. Turrell (2004), Already the day after tomorrow?, *Science*, *305*, 953–954.

Heinrich, H. (1988), Origin and consequences of cyclic ice rafting in the northeast Atlantic Ocean during the past 130,000 years, *Quat. Res.*, *29*, 142–152.

Jansen, E., and T. Veum (1990), Evidence for two-step deglaciation and its impact on North Atlantic deep-water circulation, *Nature*, *343*, 612–616.

Jansen, E., U. Bleil, R. Henrich, L. Kringstad, and B. Slettemark (1988), Paleoenvironmental changes in the Norwegian Sea and the northeast Atlantic during the last 2.8 MA: DSDP/ODP sites 610, 642, 643, and 644, *Paleoceanography*, *3*, 563–581.

Jung, S. J. A. (1996), Wassermassenaustausch zwischen NE-Atlantik und Nordmeer während der letzten 300,000/80,000 Jahre im Abbild stabiler O- und C- Isotope, Ph.D. thesis, 104 pp., Christian-Albrechts-Univ., Kiel, Germany.

Kanfoush, S. L., D. A. Hodell, C. D. Charles, T. P. Guilderson, P. G. Mortyn, and U. S. Ninnemann (2000), Millennial-scale instability of the Antarctic ice sheet during the last glaciation, *Science*, *288*, 1815–1818.

Karpuz, N. K., and E. Jansen (1992), A high-resolution diatom record of the last deglaciation from the SE Norwegian Sea: Documentation of rapid climatic changes, *Paleoceanography*, *7*, 499–520.

Keigwin, L. D. (2004), Radiocarbon and stable isotope constraints on Last Glacial Maximum and Younger Dryas ventilation in the western North Atlantic, *Paleoceanography*, *19*, PA4012, doi:10.1029/2004PA001029.

Knutz, P. C., R. Zahn, and I. R. Hall (2007), Centennial-scale variability of the British Ice Sheet: Implications for climate forcing and Atlantic meridional overturning circulation during the last deglaciation, *Paleoceanography*, *22*, PA1207, doi:10.1029/2006PA001298.

Koç, N., E. Jansen, and H. Haflidason (1993), Paleoceanographic reconstructions of surface ocean conditions in the Greenland, Iceland and Norwegian seas through the last 14 ka based on diatoms, *Quat. Sci. Rev.*, *12*, 115–140.

Kroopnick, P. (1980), The distribution of $\delta^{13}C$ in the Atlantic Ocean, *Earth Planet. Sci. Lett.*, *49*, 469–484.

Labeyrie, L., C. Waelbroeck, E. Cortijo, E. Michel, and J.-C. Duplessy (2005), Changes in deep water hydrology during the last deglaciation, *C. R. Geosci.*, *337*, 919–927.

Lambeck, K., and J. Chappell (2001), Sea level change through the last glacial cycle, *Science*, *292*, 679–685.

Levitus, S., and T. P. Boyer (1994), *World Ocean Atlas 1994*, vol. 4, *Temperature*, *NOAA Atlas NESDIS*, vol. 4, 129 pp., NOAA, Silver Spring, Md.

Liestøl, O. (1956), Glacier dammed lakes in Norway, *Nor. Geogr. Tidssk.*, *15*, 122–149.

Liu, J. P., J. D. Milliman, S. Gao, and P. Cheng (2004), Holocene development of the Yellow River's subaqueous delta, *Mar. Geol.*, *209*, 45–67.

Mackensen, A., H. W. Hubberten, T. Bickert, G. Fischer, and D. K. Fütterer (1993), The $\delta^{13}C$ in benthic foraminiferal tests of *Fontbotia wuellerstorfi* (Schwager) relative to the $\delta^{13}C$ of dissolved inorganic carbon in Southern Ocean deep water: Implications for glacial ocean circulation models, *Paleoceanography*, *8*, 587–610.

Mangerud, J., S. E. Lie, H. Furnes, I. L. Kristiansen, and L. Lømo (1984), A Younger Dryas ash bed in western Norway, and its possible correlations with tephra in cores from the Norwegian Sea and the North Atlantic, *Quat. Res.*, *21*, 85–104.

Mangerud, J., H. Furnes, and J. Johansen (1986), A 9000-year old ash bed on the Faroe Islands, *Quat. Res.*, *26*, 262–265.

Manighetti, B., I. N. McCave, M. Maslin, and N. J. Shackleton (1995), Chronology for climate change: Developing age models for the Biogeochemical Ocean Flux Study cores, *Paleoceanography*, *10*, 513–525.

Martin, S., and D. J. Cavalieri (1989), Contributions of the Siberian Shelf polynyas to the Arctic Ocean intermediate and deep water, *J. Geophys. Res.*, *94*, 12,725–12,738.

Maslin, M. (1992), A study of the paleoceanography of the N.E. Atlantic in the late Pleistocene, Ph.D. thesis, 164 pp, Univ. of Cambridge, Cambridge, U. K.

Maslin, M., N. J. Shackleton, and U. Pflaumann (1995), Surface water temperature, salinity, and density changes in the northeast Atlantic during the last 45,000 years: Heinrich events, deep water formation, and climatic rebounds, *Paleoceanography*, *10*, 527–544.

McManus, J. F., R. Francois, J.-M. Gherardi, L. D. Keigwin, and S. Brown-Leger (2004), Collapse and rapid resumption of Atlantic meridional circulation linked to deglacial climate changes, *Nature*, *428*, 834–837.

Mix, A. C., E. Bard, and R. Schneider (2001), Environmental processes of the ice age: Land, oceans, glaciers (EPILOG), *Quat. Sci. Rev.*, *20*, 627–657.

Nesje, A., and S. O. Dahl (1993), Late glacial and Holocene glacier fluctuations and climate variations in western Norway: A review, *Quat. Sci. Rev.*, *12*, 255–261.

Ninnemann, U. S., and C. D. Charles (2002), Changes in the mode of Southern Ocean circulation over the last glacial cycle revealed by foraminiferal stable isotopic variability, *Earth Planet. Sci. Lett.*, *201*, 383–396.

Nygård, A., H. P. Sejrup, H. Haflidason, M. Cecchi, and D. Ottesen (2004), Deglaciation history of the southwestern Fennoscandian Ice Sheet between 15 and 13 ^{14}C ka BP, *Boreas*, *33*, 1–17.

Oppo, D. W., and S. J. Lehman (1993), Mid-depth circulation of the subpolar North Atlantic during the Last Glacial Maximum, *Science*, *259*, 1148–1152.

Oppo, D. W., and S. J. Lehman (1995), Suborbital timescale variability of North Atlantic Deep Water during the past 200,000 years, *Paleoceanography*, *10*, 901–910.

Paul, A. and M. Schulz (2002), Holocene climate variability on centennial-to-millennial time scales: 2. Internal and forced oscillations as possible causes, in *Climate Development and History of the North Atlantic Realm*, edited by G. Wefer, W. Berger, and E. Jansen, pp. 55–73, Springer, Berlin.

Peltier, W. R. (1994), Ice age paleotopography, *Science*, *265*, 195–201.

Peltier, W. R. (2005), On the hemispheric origins of meltwater pulse 1a, *Quat. Sci. Rev.*, *24*, 1655–1671.

Peltier, W. R., and R. G. Fairbanks (2006), Global glacial ice volume and Last Glacial Maximum duration from an extended Barbados sea level record, *Quat. Sci. Rev.*, *25*, 3322–3337.

Quadfasel, D., B. Rudels, and K. Kurz (1988), Outflow of dense water from a Svalbard fjord into the Fram Strait, *Deep Sea Res., Part A*, *35*, 1143–1150.

Rasmussen, T. L., and E. Thomsen (2004), The role of the North Atlantic Drift in the millennial timescale glacial climate fluctuations, *Palaeogeogr. Palaeoclimatol. Palaeoecol.*, *210*, 101–116.

Rasmussen, T. L., E. Thomsen, T. C. E. van Weering, and L. Labeyrie (1996), Rapid changes in surface and deep water conditions at the Faeroe Margin during the last 58,000 years, *Paleoceanography*, *11*, 757–771.

Rasmussen, T., E. Thomsen, and T. C. E. van Weering (1998), Cyclic sedimentation on the Faeroe Drift 53–10 ka BP related to climatic variations, in *Geological Processes on Continental Margins: Sedimentation, Mass-Wasting and Stability*, edited by M. S. Stoker, D. Evans, and A. Cramp, pp. 255–267, Geol. Soc., London.

Rasmussen, S. O., et al. (2006), A new Greenland ice core chronology for the last glacial termination, *J. Geophys. Res.*, *111*, D06102, doi:10.1029/2005JD006079.

Risebrobakken, B., E. Jansen, C. Andersson, E. Mjelde, and K. Hevrøy (2003), A high-resolution study of Holocene paleoclimatic and paleoceanographic changes in the Nordic seas, *Paleoceanography*, *18*(1), 1017, doi:10.1029/2002PA000764.

Ruddiman, W. F., and A. McIntyre (1981), The North Atlantic during the last deglaciation, *Palaeogeogr. Palaeoclimatol. Palaeoecol.*, *35*, 145–214.

Sarnthein, M., K. Winn, S. J. A. Jung, J.-C. Duplessy, L. Labeyrie, H. Erlenkeuser, and G. Ganssen (1994), Changes in east Atlantic deepwater circulation over the last 30,000 years: Eight time slice reconstructions, *Paleoceanography*, *9*, 209–267.

Sarnthein, M., et al. (1995), Variations in Atlantic surface ocean paleoceanography, 50°–80°N: A time-slice record of the last 30,000 years, *Paleoceanography*, *10*, 1063–1094.

Schulz, H. (1995), Meeresoberflächentemperaturen vor 10.000 Jahren—Auswirkungen des frühholozänen Insolationsmaximums, Ph.D. thesis, 156 pp., Univ. of Kiel, Kiel, Germany.

Shackleton, N. J. (1974), Attainment of isotopic equilibrium between ocean water and the benthonic foraminifera genus *Uvigerina*: Isotopic changes in the ocean during the last glacial, *Colloq. Int. CNRS.*, *219*, 203–209.

Shackleton, N. J. (1987), Oxygen isotopes, ice volume and sea level, *Quat. Sci. Rev.*, *6*, 183–190.

Skinner, L. C., and N. J. Shackleton (2005), An Atlantic lead over Pacific deep-water change across Termination I: Implications for the application of the marine isotope stage stratigraphy, *Quat. Sci. Rev.*, *24*, 571–580.

Skinner, L. C., N. J. Shackleton, and H. Elderfield (2003), Millennial-scale variability of deep-water temperature and $\delta^{18}O_{dw}$ indicating deep-water source variations in the Northeast Atlantic, 0–34 cal. ka BP, *Geochem. Geophys. Geosyst.*, *4*(12), 1098, doi:10.1029/2003GC000585.

Skogseth, R., P. M. Haugan, and M. Jakobsson (2005), Watermass transformations in Storfjorden, *Cont. Shelf Res.*, *25*, 667–695.

Stuiver, M., and P. J. Reimer (1993), Extended ^{14}C data base and revised CALIB 3.0 ^{14}C age calibration program, *Radiocarbon*, *35*, 215–230.

Stuiver, M., P. M. Grootes, and T. F. Braziunas (1995), The GISP2 δ^{18}O climate record of the past 16,500 years, and the role of the Sun, ocean and volcanoes, *Quat. Res.*, *44*, 341–354.

Svendsen, J. I., A. Elverhøi, and J. Mangerud (1996), The retreat of the Barents Sea Ice Sheet on the western Svalbard margin, *Boreas*, *25, 244–256.*

Veum, T., E. Jansen, M. Arnold, I. Beyer, and J.-C. Duplessy (1992), Water mass exchange between the North Atlantic and the Norwegian Sea during the last 28,000 years, *Nature*, *356, 783–785.*

Vidal, L., L. Labeyrie, and T. C. E. van Weering (1998), Benthic δ^{18}O records in the North Atlantic over the last glacial period (60–10 kyr): Evidence for brine formation, *Paleoceanography*, *13*, 245–251.

Voelker, A. H. (1999), Zur Deutung der Dansgaard-Oeschger Ereignisse in ultra-hochauflösenden Sedimentprofilen aus dem Europäischen Nordmeer, Ph.D. thesis, 180 pp., Univ. of Kiel, Kiel, Germany.

Vogelsang, E. (1990), Paläo-Ozeanographie des Europäischen Nordmeeres an Hand stabiler Kohlenstoff- und Sauerstoffisotope, Ph.D. thesis, 136 pp., Univ. of Kiel, Kiel, Germany.

Waelbroeck, C., J.-C. Duplessy, E. Michel, L. Labeyrie, D. Paillard, and J. Duprat (2001), The timing of the last deglaciation in North Atlantic climate records, *Nature*, *412*, 724–727.

Waelbroeck, C., C. Levi, J.-C. Duplessy, L. Labeyrie, E. Michel, E. Cortijo, F. Bassinot, and F. Guichard (2006), Distant origin of circulation changes in the Indian Ocean during the last deglaciation, *Earth Planet. Sci. Lett.*, *243*, 244–251.

Weaver, A. J., J. Marotzke, P. F. Cummins, and E. S. Sarachik (1993), Stability and variability of the thermohaline circulation, *J. Phys. Oceanogr.*, *23*, 39–60.

Weinelt, M., E. Vogelsang, M. Kucera, U. Pflaumann, M. Sarnthein, A. Voelker, H. Erlenkeuser, and B. A. Malmgren (2003), Variability of North Atlantic heat transfer during MIS 2, *Paleoceanography*, *18*(3), 1071, doi:10.1029/2002PA000772.

Winton, M. (1997), The effect of cold climate upon North Atlantic Deep Water formation in a simple ocean-atmosphere model, *J. Clim.*, *39*, 37–51.

Yu, E.-F., R. Francois, and M. P. Bacon (1996), Similar rates of modern and last-glacial ocean thermohaline circulation inferred from radiochemical data, *Nature*, *379*, 689–694.

T. M. Dokken, E. Jansen, and M. Y. Meland, Bjerknes Centre for Climate Research, Allégaten 55, N-5007 Bergen, Norway. (marius.meland@bjerknes.uib.no)

K. Hevrøy, StatoilHydro Bergen, Sandslihaugen 30, Postboks 7200, N-5020 Bergen, Norway.